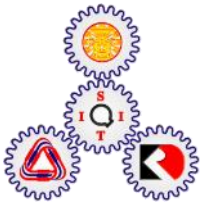

STRENGTHENING OF RC MEMBERS USING NATURAL FIBER COMPOSITES

BY

SEYHA YINH

A THESIS SUBMITTED IN PARTIAL FULFILLMENT OF THE REQUIREMENTS FOR THE DEGREE OF MASTER OF SCIENCE (ENGINEERING AND TECHNOLOGY)

SIRINDHORN INTERNATIONAL INSTITUTE OF TECHNOLOGY

THAMMASAT UNIVERSITY

ACADEMIC YEAR 2015

STRENGTHENING OF RC MEMBERS USING NATURAL FIBER COMPOSITES

BY

SEYHA YINH

A THESIS SUBMITTED IN PARTIAL FULFILLMENT OF THE REQUIREMENTS FOR THE DEGREE OF MASTER OF SCIENCE (ENGINEERING AND TECHNOLOGY)

SIRINDHORN INTERNATIONAL INSTITUTE OF TECHNOLOGY

THAMMASAT UNIVERSITY

ACADEMIC YEAR 2015

STRENGTHENING OF RC MEMBERS USING NATURAL FIBER COMPOSITES

A Thesis Presented

By

SEYHA YINH

Submitted to

Sirindhorn International Institute of Technology

Thammasat University

In partial fulfillment of the requirements for the degree of

MASTER OF SCIENCE (ENGINEERING AND TECHNOLOGY)

Approved as to style and content by

Advisor and Chairperson of Thesis Committee _____

(Assoc. Prof. Winyu Rattanapitikon, Ph.D.)

Co-Advisor _____

(Prof. Amorn Pimanmas, Ph.D.)

Committee Member and
Chairperson of Examination Committee _____

(Assoc. Prof. Manote Sappakittipakorn, Ph.D.)

Committee Member _____

(Ganchai Tanapornraweekit, Ph.D.)

MAY 2016

Acknowledgement

First and foremost, I would like to express my special gratitude and great appreciation to my advisors: Assoc. Prof. Dr. Winyu Rattanapitikon and Prof. Dr. Amorn Pimanmas for their supports throughout the process of conducting this research. Their guidance and advice were the most valuable to the success of this thesis. Undoubtedly, I could not have finished this without both of you.

Second, I would like to give my warm thanks to my thesis committee members: Assoc. Prof. Dr. Manote Sappakittipakorn and Dr. Ganchai Tanapornraweekit , for their priceless comments, suggestions and discussions, which helped me develop my research ideas into a tangible and effective.

Third, I am very grateful to acknowledge SSNC Program supported by SIIT for scholarship and thesis support. Special thanks are extended to SIIT laboratory and Asian Institute of Technology (AIT) for providing test facilities and supplying materials. Thank you Ms. Pattanun Manachitrungrueng, secretary of CET for document preparation and reimbursement.

Last but not least, I would like to thank Dr. Qudeer Hussain, for his incalculable motivating, inspiring, mentoring and instructing. You are such a phenominal person who have always been there when I needed help and support. You have shown me your sensitivity in caring for me and others. Furthermore, I am very grateful to my fellow graduate students: Mr. Shahzad Saleem, Mr. Lalin Lam and Mr. Arslan Qayyum Khan for all their help, collaboration and enthusiasm toward this research. I sincerely thank my lovely Cambodian friends: Ms. Soknim Soeng, Ms. Sovannara Chea and Ms. Sopagna Chan for their kindness and helpfulness. Thank you from the bottom of my heart for believing in me before I believed in myself.

Finally, I would like to thank my adorable parents who kindly supported me either emotional or physical strength. Both of you gave me motivation, patience and faith. I could not be more proud to be your son. Thank you very much indeed for everything. I love you and you will always be in my heart.

Abstract

STRENGTHENING OF RC MEMBERS USING NATURAL FIBER COMPOSITES

by

SEYHA YINH

Bachelor of Engineering, Faculty of Engineering, Mahasarakham University, 2013
Master of Science (Engineering and Technology), Sirindhorn International Institute of Technology, Thammasat University, 2015

This thesis is aimed to investigate the strengthening of reinforced concrete (RC) members by using externally bonded natural fiber reinforced polymers (FRP) composites. Natural FRP composites were applied to the RC members by hand lay-up method. The behavior and failure mode of strengthened specimens were experimentally investigated.

The experimental program in this study was divided into four main parts. The first part discusses the compressive behavior of small scaled concrete columns confined with sisal FRP composites jackets. Sisal fiber thickness, type of resin and concrete strength were considered as parameters. A total of 45 plain concrte cloumns were cast and tested under axial compression up to their failure. The experimental results show the efficiency of using sisal FRP composites jackets to increase load carrying capacity and ductility of concrete columns compared with the un-strengthened specimens. The comparisons between control and strengthened specimens were made and discussed in Chapter 4. The enhancement of ultimate load becomes more significant as the sisal FRP thickness was increased. The efficiency of low strength concrete with sisal FRP composites jackets is found greater than high strength concrete.

The second part presents the experiemental study conducted on the strengthening of concrete beams using sisal fiber reinforced polymer (FRP) composites. The parameters in this study were sisal fiber thickness, resin matrix (epoxy and polyester resin) and concrete strength. Six control beams and twenty four sisal FRP strengthened beams were subjected to three-point bending loads, loaded statically to ultimate failure. The results showed that Sisal FRPs are very effective to enhance the ultimate load carrying capacity and deflection of the strengthened beams compared with un-strengthened beams. The behavior and failure mode of all specimens in this group were discussed in Chapter 5. There is found an increase in ultimate load as the Sisal FRP thickness was increased for different types of concrete strengths. Both resin matrices are found effective to bond sisal FRP with concrete, however epoxy resin is found better than un-saturated polyester resin. Based on experimental results, it can be concluded that sisal FRP has a potential to increase load carrying capacity of strengthened beams.

The third part shows the series of seven reinforced concrete (RC) beams which were strengthened using externally bonded sisal FRP composites with different types of resin. All specimens were subjected to one point loading and tested up to failure. Epoxy resin and un-saturated polyester reisn were used as the adhesive to bond the concrete with Sisal FRP composites. The effects of externally bonded sisal FRP technique on the reinforced concrete (RC) beams of diffierent resin matrices and end-anchorage system were experimentally observed. The sisal FRP composites were attached at the bottom of the strengthened reinforced concrete (RC) beams . The experimental results showed that sisal FRP thickness has remarkable influences on the strengthening efficiency of externally-bonded FRP for enchancing the ultimate load of reinforced concrete (RC) beams. The behavior and failure mode of all tested beam specimens were presented and discussed in Chapter 6. The proposed epoxy anchors with steel plates is found to be significant to prevent the de-bonding of sisal FRP from concrete.

The fourth parts describes the efficiency of epoxy-bonded hemp fiber reinforced polymer (FRP) composites in flexural strengthening of reinforced concrete (RC) beams. A total of sixteen reinforced concrete (RC) beams were cast and tested under two-point loading up to failure. The test parameters included fiber thickness, strengthening configuration, anchorage system and internal reinforcement ratio. The

experimental results show the capability of hemp FRP composites to increase the loading capacity in flexure of RC beams compared with the un-strengthened beam. The enhancement of ultimate load becomes more significant as the hemp fiber thickness is increased. The effectiveness of strengthened beams in U-wrapped scheme is found greater than strengthened beams in bottom-only scheme. The propsed epoxy anchors with steel plates and hemp anchor (U-end anchor) are found to be effective to prevent the de-bonding of hemp FRP from concrete and to restore ductility of the strengthened reinforced concrete (RC) beams. The maximum increase in ultimate load of low internal reinforcement ratio group was up to 189%. Whereas the highest increase in loading capacity of high internal reinforcement ratio group was only 44.5%. Comparison in ultimate load and failure mode of all tested beam specimens were carefully investigated and discussed in Chapter 7.

Chapter 8 presents the finite element analysis carried out on reinforced concrete (RC) beams strengthened in flexure using hemp FRP composites. VecTor2 is a nonlinear finite element (FE) software which has been developed at the University of Toronto. FE program VecTor2 was used to model and analyze the reinforced concrete (RC) beams strengthened by using externally bonded hemp FRP composites. It is found that the results obtained from the VecTor2 were quite similar with the results from experiment. The finite element models has capability to predict the behavior of reinforced concrete (RC) beams especially strengthened beams using externally bonded FRP technique. This finite element program is not only effective to predict cracks at every step of loading, but also failure mode of reinforced concrete (RC) beams.

Keywords: Anchors, Concrete beams, Concrete columns, Cracks, FEM, Hemp fiber, Reinforced concrete (RC) beam, Natural fiber, Sisal fiber, Strengthening, Ultimate load

Table of Contents

List of Tables

Tables **Page**

List of Figures

Figures **Page**

Chapter 1
Introduction

1.1 General

In recent years, strengthening of new or existing reinforced concrete (RC) structures to enhance higher loading capacity or ductility has become one of the most significant studies in structural engineering society. Many strengthening techniques have been studied and developed for increasing strength capacity and enhancing stiffness of RC structures. External bonded steel plates, concrete jackets, external post-tensioning and external bonded FRP are some effective techniques, which have been successfully applied in strengthening or retrofitting of structural members. Among these techniques, externally bonded FRP is grabbing interest of numerous researchers due to the satifying properties of FRP materials. FRP composite is light weight, noncorrosive, and exhibits high tensile strength. Other advantages of FRP composite can be applied in a certain location on the concrete structures to obtain maximum efficiency.

Externally bonded FRP composite is a significant method to upgrade or retrofit the ultimate loading capacity of concrete structures. A lot of research has been studied on this technique. Nanni et al 1995 has studied concrete repair with externally bonded FRP reinforcement [1]. Rahimi et al 2001 has studied the externally bonded FRP plates strengthened concrete beams [2]. M.R. Islam et al 2005 has conducted an experimental program on shear strengthening of RC deep beams using externally bonded FRP systems [3].

Fiber reinforced polymers (FRPs) are composites consisting of reinforcing fibers together with polymer matrix. Reinforcing fibers fall into two main types, synthetic and natural fibers, each having its own properties and characteristics. The synthetic fiber such as carbon fiber is expensive and likely to cause adverse effects on environment [4] and human skin [5]. In contrast to synthetic fiber, natural fiber is environmentally friendly, cheap and locally available .

The use of natural FRP as strengthening materials has been widely used. Natural fibers (paper or cotton) were used as reinforcement in phenol resin for fabrication of large quantities of sheets, tubes and pipes as early as 1908 [6]. Several studies have

been investigated the application of natural FRP composites in structural strengthening. Wambua et al. 2003 explained that natural fiber composites have a potential to replace glass in many applications that do not require very high load bearing capabilities. Sen and Reddy 2013 has developed sisal fabric reinforced polymer, by utilizing all the FRP composites for the flexural strengthening of RC beams [7]. Sandeep Kumar L.S 2013 has studied the retrofitting of RC beams using silk FRP wrapping . Bhutta, M.A.R has conducted an experimental research on strengthening of RC beams using kenaf FRP composite laminates.

1.2 Significant of study

Based on the literature review, it was found that most research works focus on the external bonded FRP strengthening in flexure and shear of reinforced concrete (RC) members using synthetic FRP composites. Several studied focus on the strengthening of RC beams using different CFRP strips and sheets at various fiber directions [8]. Generally, RC slender beams have been used in many buildings. Once its capacity cannot withstand the current external load due to deterioration or changing of use, techniques to enhance its capacity is needed to studied and investigated. There is lack of information to understand the behavior of strengthened RC beams using external fiber composite.

1.3 Statement of problems

Existing studies have mainly conducted on strengthening of RC structures by using synthetic FRP concluded that FRP strengthening is an effective technique to enhance the ultimate load carrying capacity of the RC members. So far the work on retrofitting of structures is confined to using of carbon, glass or aramid fibers, etc., very little work is being imparted in improving structures using naturally available materials, or natural fibers. Due to its high-strength, lightweight and reasonable cost along with multidirectional fiber, improving the bonded interface between the external fibers to concrete interface using anchorage system as a method in increase the strength of RC members is needed to investigate.

1.4 Purpose of study

The objectives of this research work are as follows: (1) to investigate the compressive behavior of concrete cylinders confined with sisal FRP composites. (2) to find the suitable resin matrix which is compatible with this strengthening technique (3)

to discover suitable mechanical anchorage systems to improve the bond interface between the fiber composites and the concrete interface (4) to investigate the flexural behavior of concrete beams and RC beams strengthened with externally bonded sisal FRP composites. (5) to study the strengthening effect of RC slender beams in flexure using hemp FRP composites (6) to study the finite element analysis carried out on reinforced concrete (RC) beams strengthened in flexure using hemp FRP composites by VecTor2 .

Chapter 2
Literature Review

Fiber reinforced polymers or Fiber reinforced plastics (FRPs) are composites consisting of reinforcing fibers together with polymer matrix. Reinforcing fibers fall into two main types, synthetic and natural fibers, each having its own properties and characteristics. The most common synthetic fibers are carbon, glass, aramid fibers. They are expensive and chemically treated. Their toxic adversely affect human health and environmental sustainability. In contrast to synthetic fibers, now natural fibers are getting interest in studies for researchers. Natural fibers are biodegradable resources, low-cost and environmentally friendly products.

2.1 Review on previous strengthening methods

The recent advancement of fiber-reinforced polymer (FRP) composites as a repair and strengthening material for reinforced concrete (RC) beams, slabs and columns in structural engineering applications has increased over the past 20 years [9-12]. Extensive studies have documented that the failure of RC members strengthened with FRP was the de-bonding of FRP; making the mobilization of the full FRP tensile strength impossible in this case [13, 14]. Various materials, configurations, wrapping techniques and mechanical anchors have been explored to increase the capacity of existing RC members and postpone or delay the de-bonding process in externally bonded FRP members [14-17].

2.2 FRP confinement of concrete cylinders

Antonio Nanni and Nick M. Bradford have studied the behavior of confined concrete members by fiber reinforced plastic (FRP) materials. The dimensions of cylindrical specimens were 150 x 300 mm. Cylinders were made of normal weight and normal strength concrete. All test specimens were loaded statically under uniaxial compression up to failure. Braided aramid FRP tape, filament wound E-glass FRP, and pre-formed glass-aramid FRP shells were used as strengthening materials. Based on the experimental results, it indicates that FRP jackets effectively improve strength and pseudo-ductility of concrete [18].

Athanasios I. and Theodoros C. have studied the confinement of concrete elements using carbon FRP. Carbon FRP composites is found to be more effective than other composites due to better mechanical properites and performances. The dimensions of cylindrical specimens were 200 x 320 mm. All specimens were confinefd with carbon FRP with overlap of 160 mm. After 56 days of casting day, strengthened cylinders were subjected to axial monotonic load. According to the test results, it can be seen that using carbon FRP as external reinforcement can significantly increase the axial compression strength and ductility of concrete [19].

2.3 Flexural strengthening of reinforced concrete (RC) beams using externally bonded FRP composites

Norris et al. 1995 has performed experimental study on the flexural strengthening of reinforced concrete (RC) beams with carbon fiber sheets. Carbon fiber reinforced polymer (CFRP) were applied to the RC beams using epoxy resin as bonding agent. A total of nineteen RC beams were cast, loaded statically up to failure. Various oreintations of carbon fiber and strengthening configuration were considered as parameters as shown in Figure 2.1. Based on the results, it is found an effective increase in ultimate loading capacity and stiffness of RC beams when CFRP composites were applied to the web and tension face. A brtittle failure occurred due to lose some of ductility of strengthened RC beams [20].

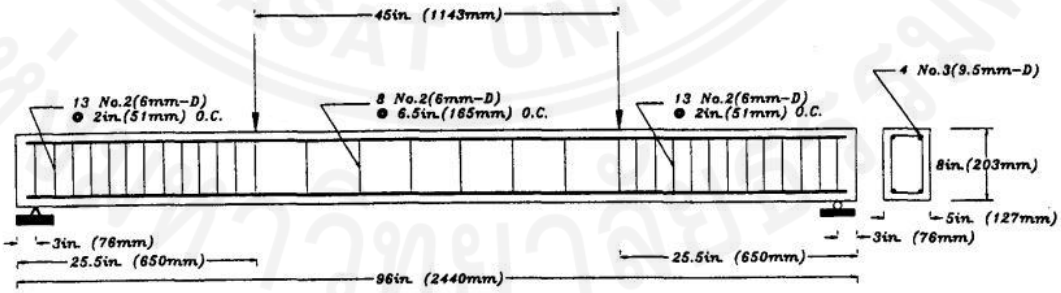

Figure 2.1 Flexural beam typical details

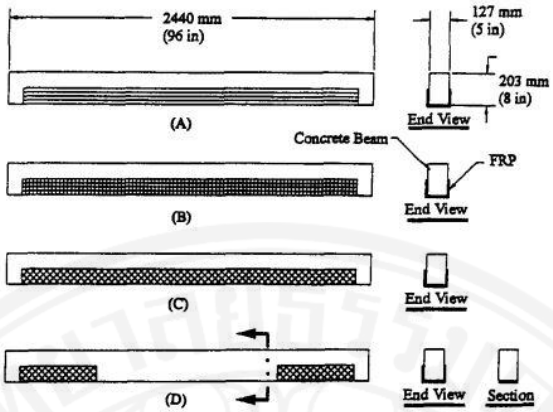

Figure 2.2 Strengthening schemes

2.4 Confinement of concrete cylinders using natural FRP jackets

Haozhi Tan et al. 2015 have studied the behavior of sisal fiber concrete cylinders externally wrapped with jute FRP. A total of 24 cylindrical specimens were cast, tested up to failure. The test parameters of this study were jute FRP wrapping thickness and sisal fiber inclusion. Jute FRP composites were used in this experimental study. The tensile strength of jute FRP composites was 83.58 approximately MPa and the tensile modulus was 2.59 GPa. The compressive behavior and failure mode of cylindrical specimens confined by jute FRP composites were experiementally investigated and recorded. Based on the results, it can be seen that jute FRP wrapping significantly enhances the loading capacity in axial compression as well as ductility of concrete cylinders. Use of jute FRP composites as external reinforcement materials might be effective to replace carbon or glass fibers [21].

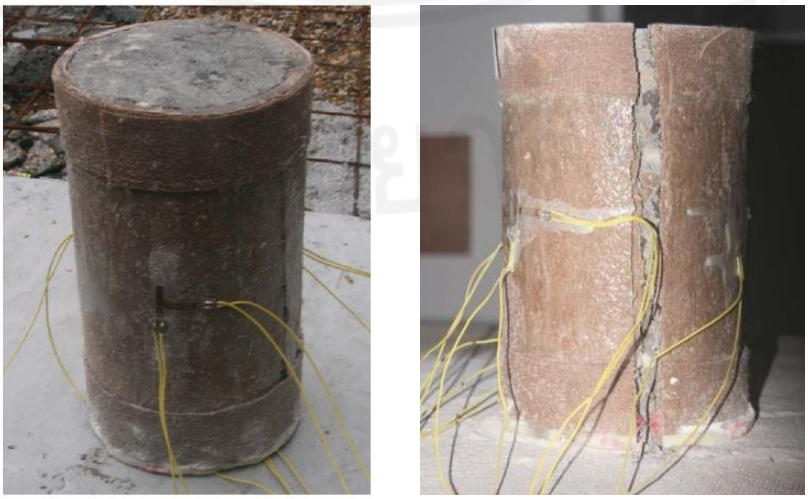

Figure 2.3 Cylinders wrapped by jute FRP

2.5 Flexural strengthening of reinforced concrete (RC) beams using externally bonded natural FRP composites

Some researchers have studied the effect of RC beams strengthened with externally bonded synthetic FRP composites in flexure [22, 23]. However, not much research has been conducted on the strengthening effect of RC beams using natural FRP composites.

Sen and Reddy 2013 has developed sisal fabric reinforced polymer by utilizing all the FRP composites for the flexural strengthening of RC beams. Sisal fiber reinforced polymer (SFRP) composites were investigated and compared to carbon fiber reinforced polymer (CFRP) and glass fiber reinforced polymer (GFRP) composites. Reinforcement details of RC beams are provided in Figure 2.5.

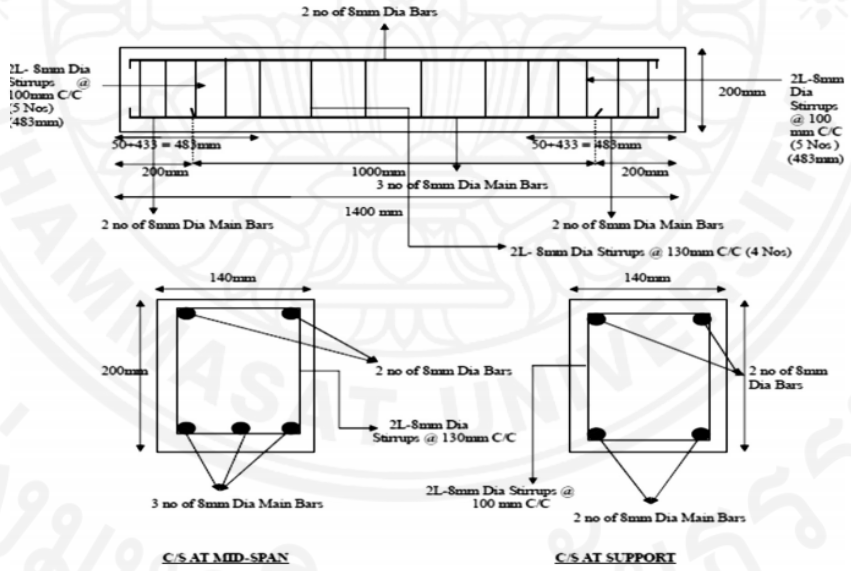

Figure 2.4 Typical details of RC beam specimen

Failure modes and strengthening effect of SFRP on RC beams were carefully observed. RC beams were strengthened with SFRP, CFRP and GFRP composites in U-wrap scheme with two different techniques, i.e. full and partial wrapping. All specimens were subjected to third-point loading accordance to ASTM C78/C78M as shown in Figure 2.4 [7].

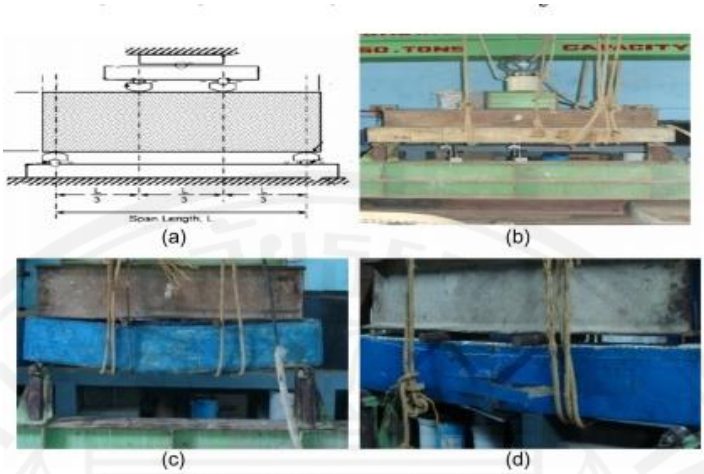

Figure 2.5 Three-point loading set up

Sandeep kumar L.S 2013 has studied the retofitting of RC beams using silk FRP wrapping. Silk is a natural fiber which can be matted, knitted and woven into texiles. The tensile strength and modulus of elasticity of silk fiber were 130 MPa and 9 GPa, respectively. A total of five RC beams were cast and tested up to failure. According to the results, the ultimate load was found to be high for beams retrofitted with NSFRP (silk) composites as compared to control beam. The flexural strengthening made the RC beams stronger and stiffer [24].

Bhutta, M.A.R. 2013 has conducted an experimental research program on the strengthening of RC beams using externally bonded kenaf fiber reinforced polymer composite laminates. A total of eight RC beams, six of them were strengthened by kenaf FRP with different types of resin matrix i.e. epoxy, polyester and vinyl ester resin, the remaining two RC beams were not strengthened and served as control specimens. Beam dimension is given in Figure 2.6. The control beams failed in normal failure mode of orinary RC beam. Whereas all six strengthened RC beams failed due to rupture of composites laminates. Failure modes of tested beams are shown in Figure 2.7. It is found an increase in flexural strength approximately about 40% compared to control beams.

All evidences indicate that kenaf FRP composites can be used as strengthening materials for RC beams [25].

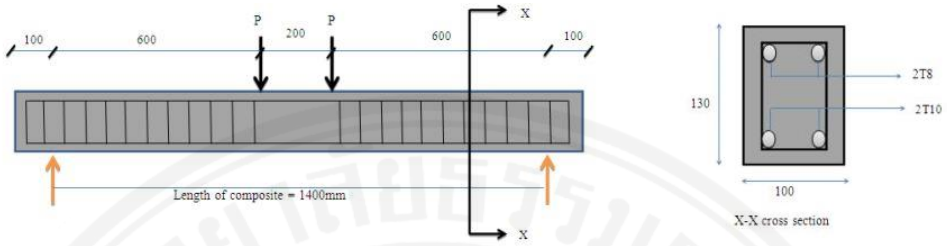

Figure 2.6 Beam dimension

Figure 2.7 Failure modes of tested RC beams

Md. Ashraful Alam. 2015 has studied the flexural strengthening of reinforced concrete (RC) beam using jute rope composite plate. Jute rope is a great material for fabricating a plate. Fabricating of jute rope composite plate is presented in Figure 2.8.

Figure 2.8 Fabricating of jute rope composite plate

A total of two RC beams, one was strengthened by jute rope composite plate, and the remaining one was served as control specimen. Beam dimension is provided in Figure 2.9. All beams are subjected to two point loading conditions using Universal Testing Machine (UTM). Instrumentation and test set up of specimens is shown in Figure 2.10 .

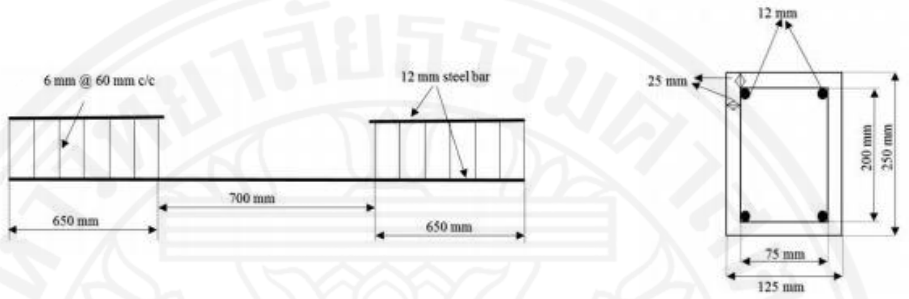

Figure 2.9 Reinforcement details of beam specimens

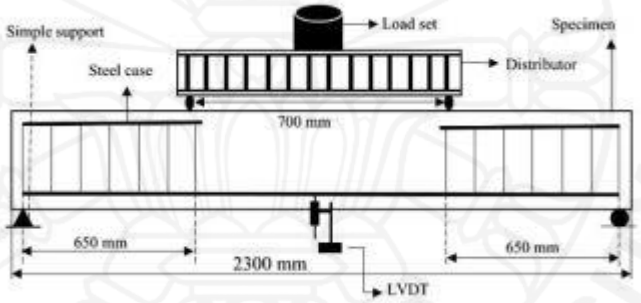

Figure 2.10 Instrumentation and test set up of specimens

From the experiemental results, it it found that jute rope composite plate enchances the loading capacity of strengthened RC beam up to 58% compared with control specimen [26].

Chapter 3
Material Properties

3.1 Concrete materials

Concrete is a basic composite material composed of cement, fine aggregate, coarse aggregates and water. Properties and characteristics of concrete components are presented in this chapter.

3.1.1 Cement

Cement was manufactured by Siam Cement Group Co. Ltd. The cement is classified as Type 1, Normal Portland Cement.

3.1.2 Fine aggregates (sand)

Fine aggregates used in this study was saturated surface dry (SSD) clean river sand with a fineness modulus of approximately 2.55. It was purchased from Rung Sin Co. Ltd., Thailand which has a relative density of 2.75.

3.1.3 Coarse aggregates (gravel)

Coarse aggregates used in this study was crushed gravels with a maximum size of 19 mm . The aggregates were also purchased from Rung Sin Co. Ltd., Thailand. The relative density and SDD absorption values were 2.71 and 1.24%, respectively. The dry rodded density of gravels was 1,555 kg/m^3.

3.1.4 Water

Water was taken directly from Rangsit waterworks authority. Concrete mixing was prepared in the SET laboratory (AIT).

3.2 Reinforcing steel bars

Reinforcing steel bars were obtained from Rung Sin Co. Ltd., Thailand. The mechanical properties of all reinforcing steel bars are provided in Table 3.1.

Table 3.1 Mechanical properties of stirrups and rebars

Type	Yield strength (MPa)	Ultimate tensile strength (MPa)
RB6	313	500
RB9	420	570
DB10	439	580
DB16	547	700

3.3 Resin sytem

3.3.1 Epoxy resin

The epoxy which was used as a matrix resin in this experimental program was provided by Smart and Bright Co., Ltd, Thailand under the product name “SMART CF-RESIN”. SMART CF-RESIN is a solvent free (100% solid) two part high performance epoxy resin. It consisted of two parts; i.e., resin (Part A) and hardener (Part B). SMART CF-RESIN uses 2 parts of resin to 1 parts of hardener by weight, which is recommended by the manufacturer. It was mixed by using a fast-speed drill mix for at least 3-4 minutes until solution becomes homogeneous. The mechanical properties of the epoxy resin were detailed in Table 3.2.

Figure 3.1 Epoxy resin

Table 3.2 Mechanical properties of epoxy resin

Properties		
Solid content	100%	
Pot life at 25°C	40 – 60 minutes	
Curing time	7 – 10 hours	
Mixed ratio	A : B = 2 : 1 by weight	
Compression strength	650 kgf/cm^2	(ASTM C109)
Tensile strength	50 MPa	(ASTM D638)
Elongation at break	2.5%	(ASTM D638)

Flexural strength	75 MPa	(ASTM D790)
Bond strength	2.11 N/mm^2	(Pull off test)
Thermal conductivity	0.083 W/m°K	(ASTM C177)

3.3.2 Un-saturated polyester resin

Un-saturated polyester resin was manufactured by Dongguan Tiger Fiber Glass Co., Ltd . The tensile strength and tensile modulus of polyester resin were 145 MPa and 12.8 GPa, respectively. Its elongation was 1.5 %. This mechanical properties was provided by Polyline Company. This polyester resin consisted of two parts; i.e., resin (Part A) and hardener (Part B). The mixing proportion ratio was 100:1 by weight, respectively.

Figure 3.2 Polyester resin

3.4 Sisal fiber reinforced polymer (FRP) compsoites

3.4.1 Material properties of Sisal FRP composites

Sisal fibers were obtained from farms in Cha Am district, Thailand. They were extracted from the sisal plant leaves in the form of long fiber bundles. Sisal FRP composites were made from sisal fiber together with resin matrix by using hand-layup method. The applying process and strengthening procedure are explained in the following section. The mechanical properties of sisal FRP composites are discussed below.

3.4.2 Density

The density is determinded by following ASTM Standard D792 [27].

3.4.3 Tensile properties of sisal FRP composite

The tensile strength of sisal FRP composites were determined by testing the strip specimens of sisal FRP in accordance with ASTM Standard D638 [28]. The mechanical properties of sisal FRP composites are given in Table 3.3 and 3.4.

Figure 3.3 Tensile strength testing of hemp FRP composites

Table 3.3 Mechanical properties of sisal FRP composites using epoxy resin

Properties	Value	Units
Tensile strength	104	MPa
Density of sisal FRP	2.81	g/cm^3
Fracturing strain	0.41	%
Ultimate strain	3.48	%
Modulus of elasticity	3.19	GPa

Table 3.4 Mechanical properties of sisal FRP composites using polyester resin

Properties	Value	Units
Tensile strength	80	MPa
Density of sisal FRP	2.88	g/cm^3
Fracturing strain	0.51	%
Ultimate strain	3.65	%
Modulus of elasticity	3.02	GPa

3.5 Hemp fiber reinforced polymer (FRP) compsoites

3.5.1 Material properties of Hemp FRP composites

Hemp fibers were obtained from farms in Khon Kaen province, Thailand. They were extracted from the hemp plant leaves in the form of long fiber bundles. Hemp FRP composites were made from hemp fiber together with resin matrix by using hand-layup method. The applying process and strengthening procedure are explained in the following section. The mechanical properties of hemp FRP composite are discussed below.

3.5.2 Density and fracturing strain

The density and fracturing strain are determinded by following ASTM Standard D792 [27] and ASTM Standard D2584 [29], respectively.

3.4.3 Tensile properties of hemp FRP composite

The tensile strength of sisal FRP composites fiber were determined by testing the strip specimens of sisal FRP in accordance with ASTM Standard D638 [28]. The mechanical properties of GCSM composite are given in Table 3.5.

Figure 3.4 Tensile strength testing of hemp FRP composite

Table 3.5 Mechanical properties of hemp FRP composites using epoxy resin

Properties	Value	Units
Tensile strength	156	MPa
Density of hemp FRP	2.65	g/cm^3
Fracturing strain	0.505	%
Ultimate strain	2.035	%
Modulus of elasticity	6.414	GPa

Chapter 4

Compressive Behavior of Concrete Columns Confined by Sisal Fiber Reinforced Polymer (FRP) Composites

4.1 General

This chapter describes the efficiency of externally bonded sisal fiber reinforced polymer (sisal FRP) composites in confinement of concrete columns. The objectives of this study are to examine the compressive behavior of plain concrete columns confined by sisal FRP as reinforcement and to investigate the failure modes of sisal FRP confined concrete columns. Sisal fiber thickness and concrete strength were considered as parameters. The experimental results showed the efficiency of using polyester-bonded sisal FRP to increase the load carrying capacity in axial compression of concrete columns compared with the un-strengthened specimens.

4.2 Experimental program

4.2.1 Specimen details and test setup

The typical details of test specimens are shown in Figure 4.1 and test matrix is summarized in Table 4.1. The cylinder dimensions are 200 mm long and 100 mm in diameter. It is devided into 3 groups (A, B and C) based on concrete strength. A total of 45 cylinders were tested,out of 9 cylinders which were not confined by sisal FRP composites, served as control specimens (3 cylinders per each group). The remaining cylinders were confined with different sisal fiber thickness (i.e. 1 or 2 layers). Cylindrical specimens were confined in axial compression. Sisal fiber thickness, resin matrix and concrete strength were considered as parameters. The strengthening performed using different resin matrix (i.e. un-saturated polyester and epoxy resin) as bonding agent between sisal FRP composites and concrete. In the experimental program, cylindrical specimens were tested under static axial loading up to failure in universal tesing machine (UTM) of capacity 2000 kN at a constant rate of 4 N per second. Applied loads and failure modes were carefully observed. Linear variable displacement transducers (LVDTs) were used to measure deformation of cylindrical specimens. Test setup and instrumentation of all specimens are shown in Figure 4.2. The specimen notations are assigned to identify research parameters.

For example in specimen C-L-P-1L, first letter represents cylindrical specimen. Second letter stands for low strength concrete, Third letter decribes resin matrix i.e. polyester resin and the last number indicates sisal FRP thickness i.e. 1 layer.

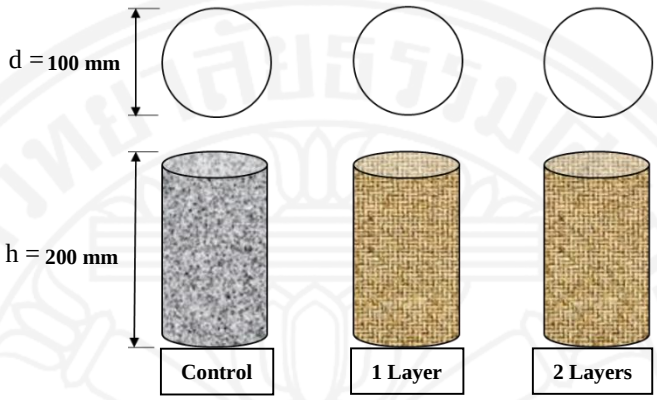

Figure 4.1 Details of specimens

Table 4.1 Test matrix and designation

Group	Designation	Concrete strength	Resin Matrix	Fiber thickness (layers)	Number of specimens
A	C-L-CON	Low strength	-	-	3
	C-L-P-1L	Low strength	Polyester	1	3
	C-L-P-2L	Low strength	Polyester	2	3
	C-L-E-1L	Low strength	Epoxy	1	3
	C-L-E-2L	Low strength	Epoxy	2	3
B	C-M-CON	Medium strength	-	-	3
	C-M-P-1L	Medium strength	Polyester	1	3
	C-M-P-2L	Medium strength	Polyester	2	3
	C-M-E-1L	Medium strength	Epoxy	1	3
	C-M-E-2L	Medium strength	Epoxy	2	3
C	C-H-CON	High strength	-	-	3
	C-H-P-1L	High strength	Polyester	1	3
	C-H-P-2L	High strength	Polyester	2	3
	C-H-E-1L	High strength	Epoxy	1	3
	C-H-E-2L	High strength	Epoxy	2	3

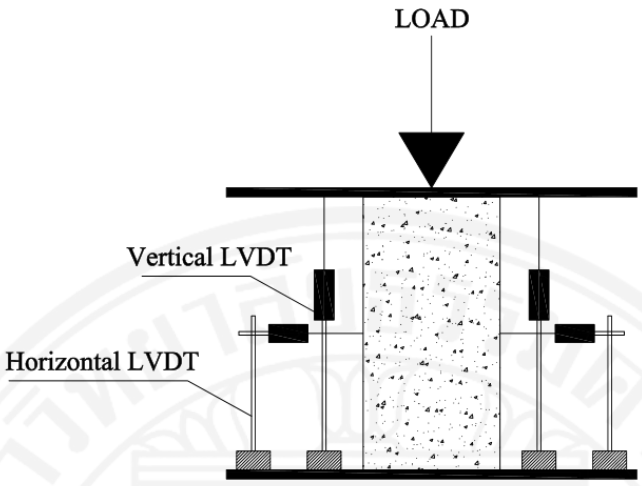

Figure 4.2 Loading set-up

4.2.2 Material Properties

On the testing day (30-40 days) the compressive strengths of LS, MS and HS concrete were 19 MPa, 38 MPa and 58 MPa, respectively. Mix proportions are given in Table 4.2. Sisal fiber is a natural fiber extracted from the leaves of sisal plants which is locally available in the north and south of Thailand. Raw sisal fiber is mostly used for making fashion accessaries and household ítems. It can be knitted and spun into filaments. In this experimental study, un-saturated polyester resin and epoxy resin were used to bond sisal fiber with concrete. The tensile strength of sisal FRP with epoxy and polyester resin were approximately 104 MPa and 80 MPa, respectively. Mechanical properties of sisal FRP composites are provided in Table 4.3.

Table 4.2 Concrete mix composition (per cubic meter)

Components (kg/m^3)	LS	MS	HS
Cement	241	402	509
Water	213	183	206
Sand	788	755	842
Gravel	1158	1060	842

Table 4.3 Machanical Properties of sisal FRP composites

Properties	Sisal FRP using polyester resin	Sisal FRP using epoxy resin	Units
Tensile strength	80	104	MPa
Tensile modulus	3.02	3.19	GPa
Fracturing strain	0.51	0.41	%
Density	2.88	2.81	g/cm^3

4.2.3 Stregthening process

All specimens were cast on the same day and kept for 28 days in the temperature and humidity controlled room before applying sisal FRPs. Sisal fibers were pre-treated (4-6 hours) using sun light to remove moisture. The confinement of concrete cylinders using sisal FRP was performed using hand layup process as shown in Figure 4.3. Sisal FRP was confined around the whole circumference of the concrete cylinders. 1 or 2 layers for each uni-directional fabric were employed. Seven days after the lay-up process, all cylindrical specimens were then subjected to uni-axial compression test, respectively.

Figure 4.3 FRP wrapping procedure for cylindrical specimens

4.3 Results and discussions

Table 4.4 Results of tested specimens

Group	Specimen designation	Peak load (kN)	% Increase in peak load	Deformation against peak load (mm)	% Increase in deformation
A	C-L-CON	17.21	-	1.77	-
	C-L-P-1L	26.86	56	5.61	217
	C-L-P-2L	35.00	103	7.68	334
	C-L-E-1L	31.72	84	5.03	184
	C-L-E-2L	46.95	173	5.83	229
B	C-M-CON	32.82	-	1.34	-
	C-M-P-1L	40.64	24	3.90	191
	C-M-P-2L	47.97	46	5.30	295
	C-M-E-1L	45.35	38	3.08	130
	C-M-E-2L	58.17	77	5.83	335
C	C-H-CON	46.00	-	1.69	-
	C-H-P-1L	52.50	14	2.26	34
	C-H-P-2L	54.45	18	3.31	96
	C-H-E-1L	56.10	22	2.81	66
	C-H-E-2L	59.17	29	4.79	183

The control specimen of group A (low strength), C-L-CON failed at the load of 17.21 kN. C-L-P-1L and C-L-P-2L failed at the peak loads of 26.86 kN and 35 kN, which were 56% and 103% higher than control cylinder (CL-CON), respectively. Whereas C-L-E-1L and C-L-E-2L failed at the ultimate loads of 31.72 kN and 46.95 kN, which were 84% and 173% increased compared with C-L-CON. The load-deformation curves of low strength group of cylindrical specimens are provided in Figure 4.4.

The control specimen of group B (medium strength), (C-H-CON) failed at the ultimate load of 32.82 kN. Whereas confined cylindrical specimens C-M-P-1L, C-M-P-2L, C-M-E-1L and C-M-E-2L failed at 24%, 46%, 38% and 77% higher ultimate load compared with control cylinder, respectively. The load-deformation curves of medium strength group of cylindrical specimens are provided in Figure 4.5.

The control specimen of group C (high strength), (C-H-CON) failed at the ultimate load of 46 kN. The results showed that the increase in the ultimate load-carrying capacities of confined specimens C-H-P-1L and C-H-P-2L were 14% and 18%, respectively. 22% and 29% increases in ultimate load-carrying capacity were obtained

for beams C-H-E-1L and C-H-E-2L, respectively. The load-deformation curves of high strength group of cylindrical specimens are provided in Figure 4.6.

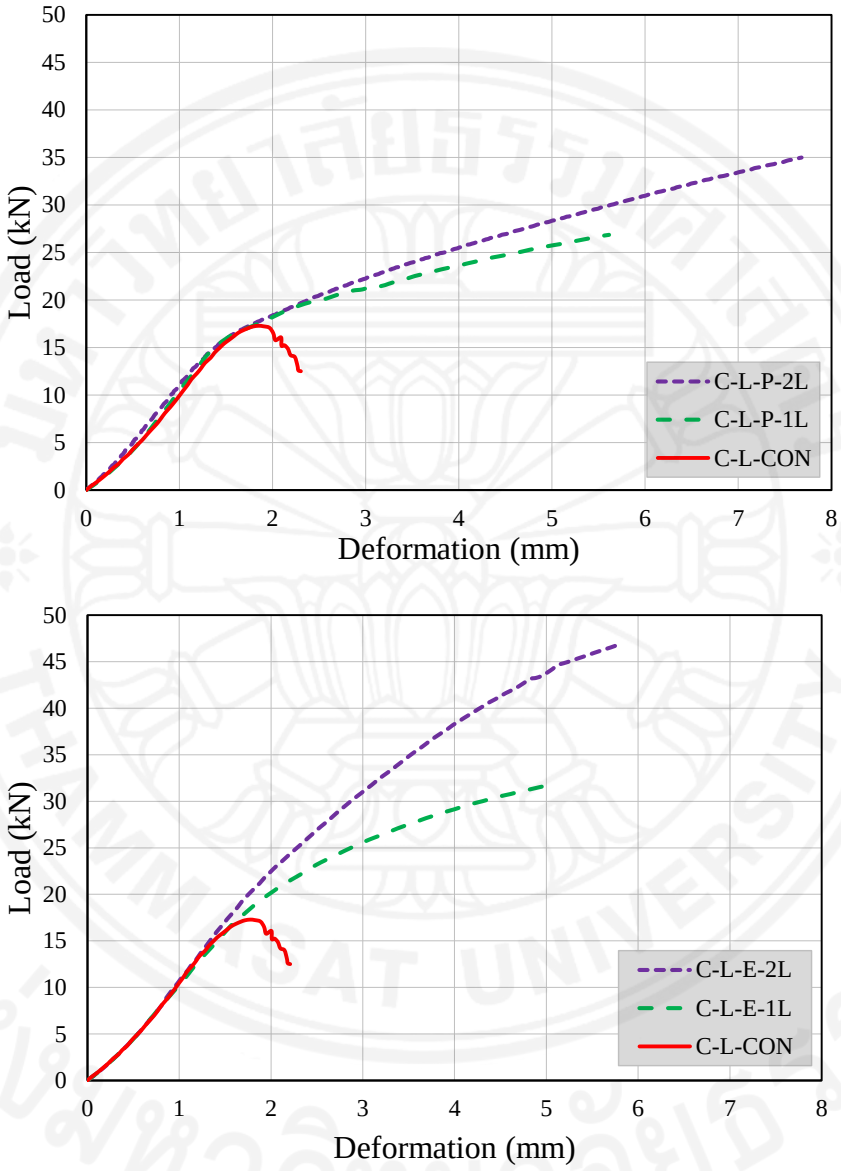

Figure 4.4 Load-deformation curves of tested cylindrical specimens group A

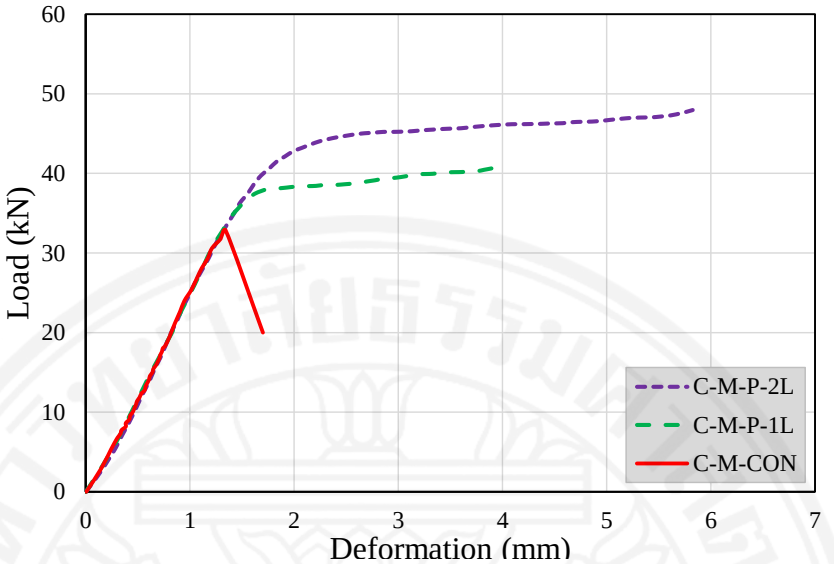

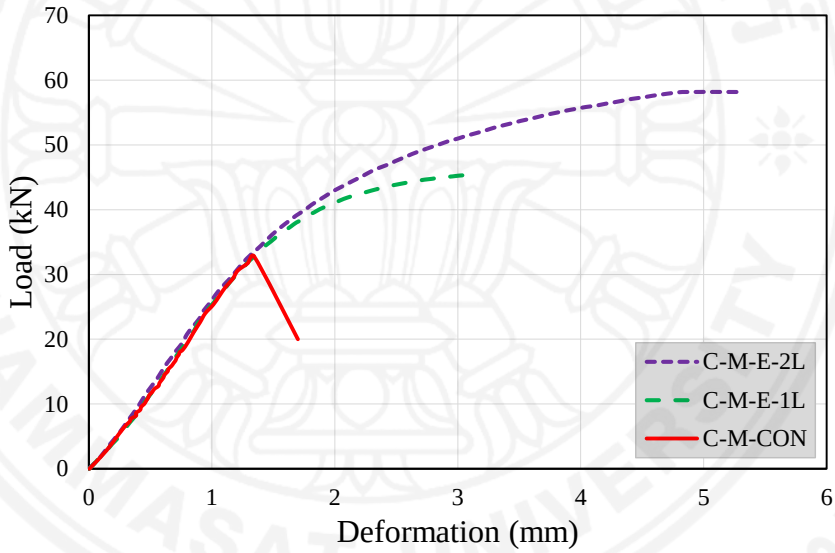

Figure 4.5 Load-deformation curves of tested cylindrical specimens group B

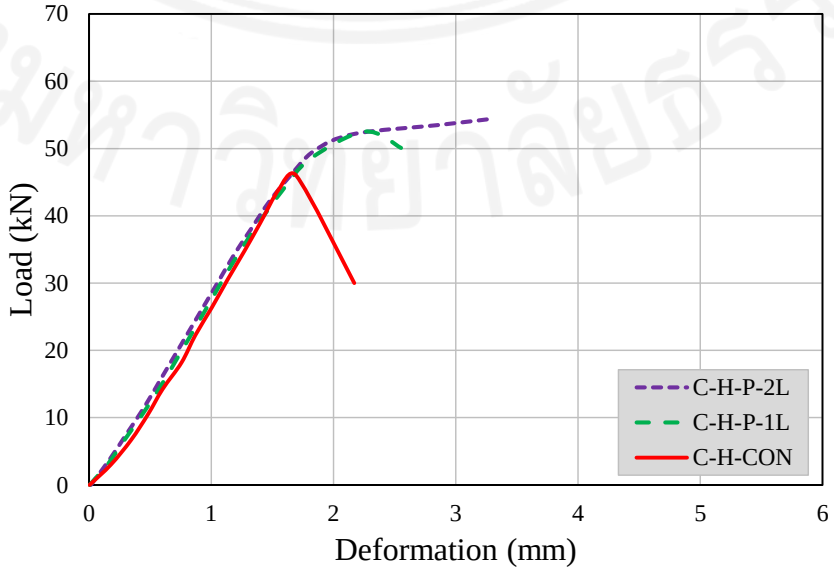

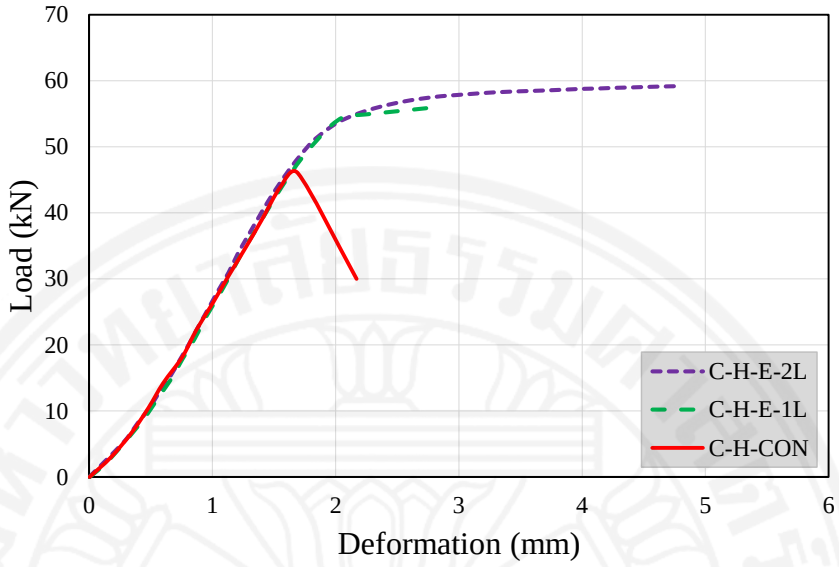

Figure 4.6 Load-deformation curves of tested cylindrical specimens group B

4.3.1 Effect of test parameters

Fiber thickness, resin matrix and concrete strength were the test parameters in this experimental study. In order to investigate the effect of these parameters, a comparison of ultimate loads is drawn among different cylindrical specimens as shown in Figure 4.7. In this comparison graph, Y-axis is representing percentage increase in ultimate load with respect to the control column in each group. As can be seen that sisal FRP strengthening has significant effect on ultimate load carrying capacity of strengthened concrete columns. There is found increase in load carrying capacity as the fiber thickness was increased. Both resin matrices are found suitable to bond sisal FRP with concrete, however epoxy resin is found better in performance compared with olyester resin. The efficiency of externally bonded sisal FRPs are found lower for high strength concrete.

4.3.2 Failure modes

All circular sisal FRP composites confined specimens were failed by rupture of sisal FRP jackets due to hoop tension. The final failure of confined specimens was corresponding to the rupture of sisal FRP jackets as shown in Figure 4.8. The rupture of epoxy coated sisal FRP jackets was explosive with large sounds whereas the failure of polyester coated sisal FRP jackets was not explosive. However, clear snapping sounds were observed in almost all sisal FRP confined specimens prior to the rupture.

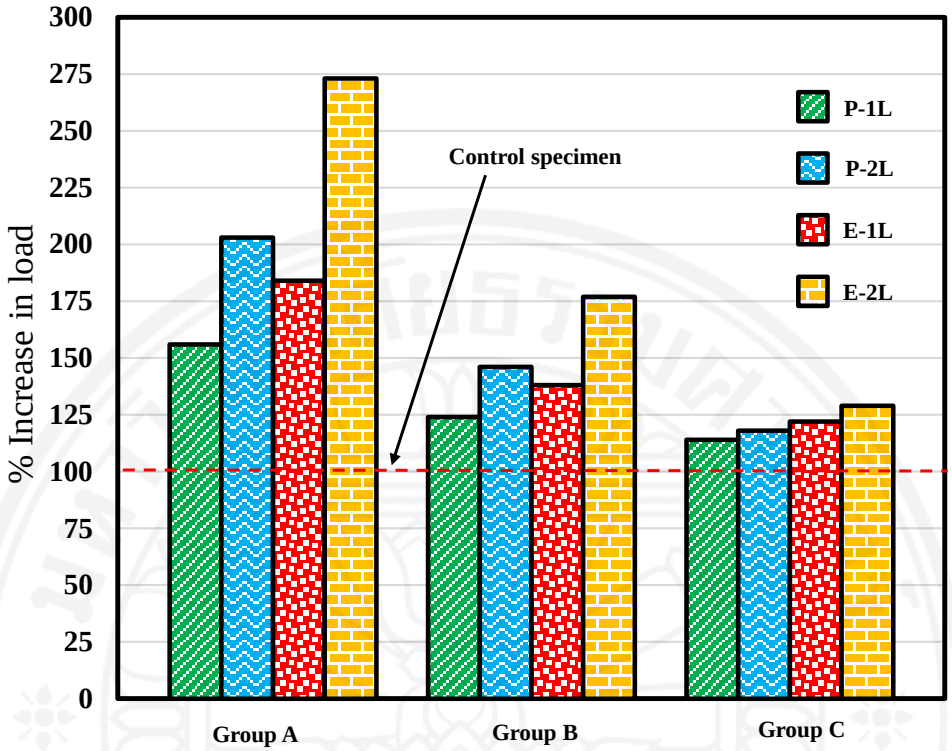

Figure 4.7 Comparison in ultimate load

(a) (b)

Figure 4.8 Typical failure modes of cylinder specimen; (a) control un-strengthened, (b) NFRP strengthened

4.4 Conclusions

This chapter presents results from an experimental study conducted on externally bonded sisal FRP strengthening of concrete columns. Fiber thickness resin

matrix and concrete strength were the necessary test parameters in this study. The findings showed that sisal-FRP-strengthened cylindrical specimens exhibit significantly higher load-carrying capacity than the control specimens. There is also found an increase in ductility of concrete columns. Fiber thickness, resin matrix and concrete strength have remarkable influences on the ultimate load of all confined specimens. The enhancement of ultimate load becomes more significant as the sisal FRP thickness is increased. The efficiency of low strength concrete with externally bonded-sisal FRP is found greater than medium and high strength concrete. Both resin matrices are found suitable to bond sisal FRP with concrete, however epoxy resin is found better in performance compared with polyester resin due to better mechanical properties. Based on the results, it can be concluded that using sisal FRP as a strengthening material may be effective and advantageous because it has a great potential to enhance the compressive strength of plain concrete columns. For the further study should be carried out to investigate the strengthening effect of sisal FRP jackets on square or rectangular concrete columns.

Chapter 5
Strengthening Effect of Sisal Fiber Reinforced Polymer (FRP) Composites on Concrete Beams

5.1 General

This chapter presents an experimental study on the strengthening of concrete beams using sisal fiber reinforced polymer (sisal FRP) composites, which are a specific type of natural-fiber-based polymer materials. Sisal FRPs are both economically and ecologically attractive materials, utilized effectively for making low-cost construction and maintenance. The parameters in this study were sisal fiber thickness, resin matrix (epoxy and polyester resin) and concrete strength. six control beams and twenty four sisal FRP strengthened beams were subjected to three-point bending loads, loaded statically to ultimate failure. The load-mid-span-deflection curves of strengthened beam specimens were plotted against that of control specimen to observe the effect of test parameters on the behavior of concrete beams. The failure modes of all tested beam specimens were carefully observed and discussed in this chapter.

5.2 Experimental program

5.2.1 Specimen details and test matrix

The dimensions of the test specimen were 100 x 100 x 500 mm as shown in Fig. 1. All specimens were prepared using wood molds made using plywood sheets. Oil was applied to the plywood sheets prior to the concerting to facilitate de-molding. A total of 30 plain concrete beams were cast using different concrete strengths. Ten of them were made from low strength (LS) concrete, another 10 made from medium strength (MS) concrete and remaining 10 were made from high strength (HS) concrete. Test matrix is divided into three groups based on concrete strength as shown in Table 5.1. In each group two beam were served as control or un-strengthened beams whereas remaining beams were strengthened with sisal FRP. The specimen notations are assigned to identify research parameters. For example in beam specimen B-L-P-2L, first letter represents beam specimen, second letter stands for concrete strength i.e. low strength concrete. Third letter examines resin matrix i.e. polyester resin and last number indicates sisal FRP thickness i.e.2 layers of fiber.

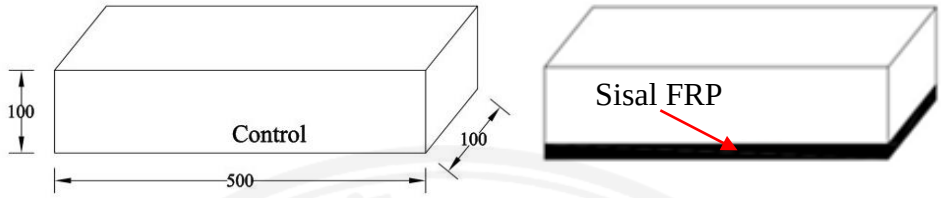

Figure 5.1 Details of test specimens (unit in mm)

Table 5.1 Test matrix

Group	Designation	Concrete strength	Resin Matrix	Fiber thickness (layers)	Number of specimens
A	B-L-CON	Low strength	-	-	2
	B-L-P-1L	Low strength	Polyester	1	2
	B-L-P-2L	Low strength	Polyester	2	2
	B-L-E-1L	Low strength	Epoxy	1	2
	B-L-E-2L	Low strength	Epoxy	2	2
B	B-M-CON	Medium strength	-	-	2
	B-M-P-1L	Medium strength	Polyester	1	2
	B-M-P-2L	Medium strength	Polyester	2	2
	B-M-E-1L	Medium strength	Epoxy	1	2
	B-M-E-2L	Medium strength	Epoxy	2	2
C	B-H-CON	High strength	-	-	2
	B-H-P-1L	High strength	Polyester	1	2
	B-H-P-2L	High strength	Polyester	2	2
	B-H-E-1L	High strength	Epoxy	1	2
	B-H-E-2L	High strength	Epoxy	2	2

5.2.2 Material Properties

On the testing day (28 days) the compressive strengths of LS, MS and HS concrete were 19 MPa, 38 MPa and 58 MPa, respectively. Mix proportions are given in Table 5.2. Sisal fiber is a natural fiber extracted from the leaves of sisal plants which is locally available in the north and south of Thailand. Raw sisal fiber is mostly used for making fashion accessaries and household ítems. It can be knitted and spun into filaments. In this experimental study, un-saturated polyester resin and epoxy resin were used to bond sisal fiber with concrete. The tensile strength of sisal FRP with epoxy and polyester resin were approximately 104 MPa and 80 MPa, respectively. Mechanical properties of sisal FRP composites are provided in Table 5.3.

Table 5.2 Mix proportions

Components (kg/m^3)	LS	MS	HS
Cement	241	402	509
Water	213	183	206
Sand	788	755	842
Gravel	1158	1060	842

Table 5.3 Mechanical properties of sisal FRP composites

Properties	Sisal FRP using polyester resin	Sisal FRP using epoxy resin	Units
Tensile strength	80	104	MPa
Tensile modulus	3.02	3.19	GPa
Fracturing strain	0.51	0.41	%
Density	2.88	2.81	g/cm^3

5.2.3 Strengthening process

All specimens were cast on the same day and kept for 28 days in the temperature and humidity controlled room before applying sisal FRPs. Sisal fibers were pre-treated (4-6 hours) using sun light to remove moisture. The concrete surface that will receive fiber were cleaned to remove any debris and dust. Sisal FRPs were applied on the bottom surface of concrete specimens.

Figure 5.2 Hand layup process

5.2.4 Test setup and instrumentation

All specimens were subjected to three-point bending loads, loaded statically to ultimate failure as shown in Fig. 3. The load was applied at a constant rate of 100N/minute. The beam deflection was recorded using LVDT at the mid span. The applied loads and corresponding deflections were carefully measured.

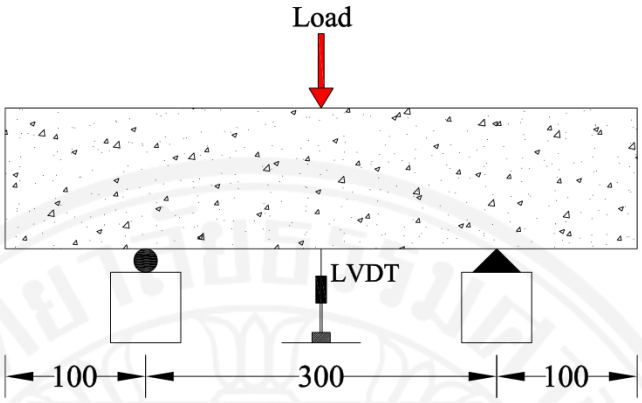

Figure 5.3 Loading set-up (unit in mm)

5.3 Results and discussions

Table 5.4 Test results

Group	Specimen designation	Ultimate load (kN)	Increase in ultimate load (%)	Mid span deflection against peak load (mm)
A	B-L-CON	9.04	-	0.20
	B-L-P-1L	25.20	179	2.10
	B-L-P-2L	34.85	286	2.38
	B-L-E-1L	39.26	334	1.68
	B-L-E-2L	55.77	517	1.95
B	B-M-CON	10.75	-	0.16
	B-M-P-1L	25.77	140	2.08
	B-M-P-2L	38.24	256	2.15
	B-M-E-1L	28.35	164	1.81
	B-M-E-2L	45.78	326	1.96
C	B-H-CON	13.50	-	0.09
	B-H-P-1L	25.30	87	1.91
	B-H-P-2L	32.15	138	1.83
	B-H-E-1L	30.43	125	1.80
	B-H-E-2L	47.98	255	1.98

Control beam (B-L-CON) of group A failed suddenly at the load of 9.04 kN. The results showed that the increase in the ultimate loading capacities of sisal FRP strengthened beams using polyester resin i.e. B-L-P-1L and B-L-P-2L were 179% and 286%, respectively (compared with control beam). Beam B-L-E-1L and B-L-E-2L were strengthened using polyester resin. These beams i.e. B-L-E-1L and B-L-E-2L, failed at the peak loads of 39.26 kN and 55.77 kN which were 334% and 517% higher than control

beam. The load-mid span deflection curves of low strength group are provided in Figure 5.4.

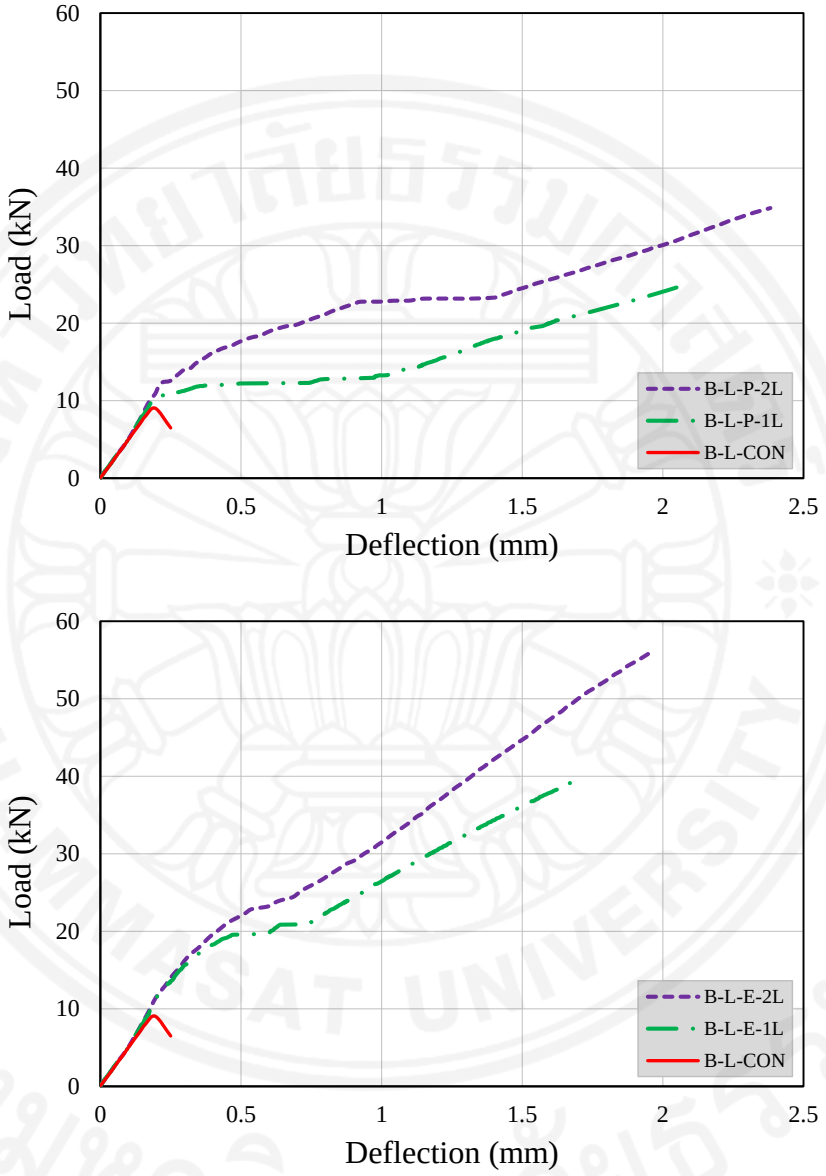

Figure 5.4 Load-mid span deflection curves of beam specimens group A

The control beam (B-M-CON) of group B failed abruptly at ultimate load of 10.75 kN, slightly higher load than beam B-L-CON due to higher strength of concrete. Sisal FRP strengthened beams showed significant increase in ultimate load carrying capacity and mid span deflection. 140% and 256% increases in ultimate load carrying capacity were recorded for beams HS-3P and HS-6P, respectively. Whereas beam specimens B-M-E-1L and B-M-E-2L were failed at 164% and 326% higher ultimate load

compared with control beam, respectively. The load-mid span deflection curves of medium strength group are provided in Figure 5.5.

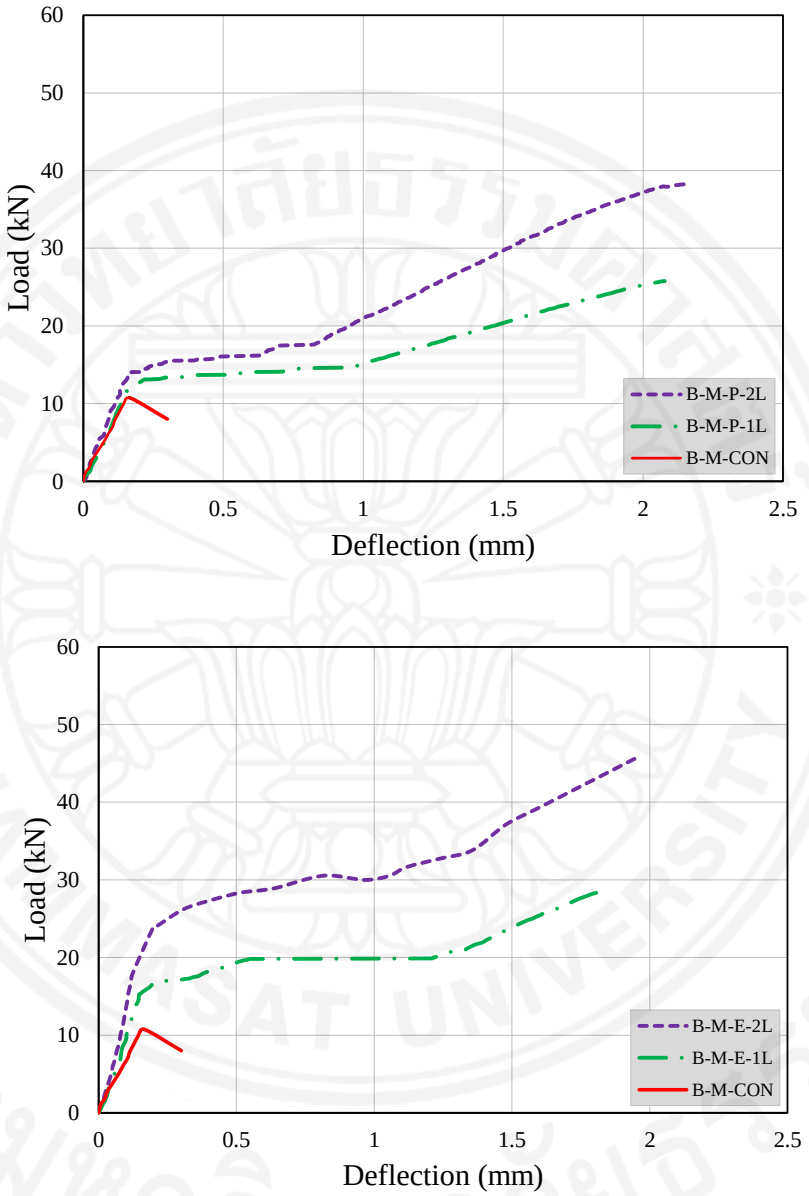

Figure 5.5 Load-mid span deflection curves of beam specimens group B

The control specimen of group C (high strength), (B-H-CON) failed at the ultimate load of 13.5 kN. The results showed that the increase in the ultimate load-carrying capacities of polyester-bonded sisal FRP strengthened specimens B-H-P-1L and B-H-P-2L were 87% and 138%, respectively. 125% and 255% increases in ultimate load-carrying capacity were obtained for epoxy-bonded sisal FRP strengthened beams B-H-

E-1L and B-H-E-2L, respectively. The load-deformation curves of high strength group are provided in Figure 5.6**.**

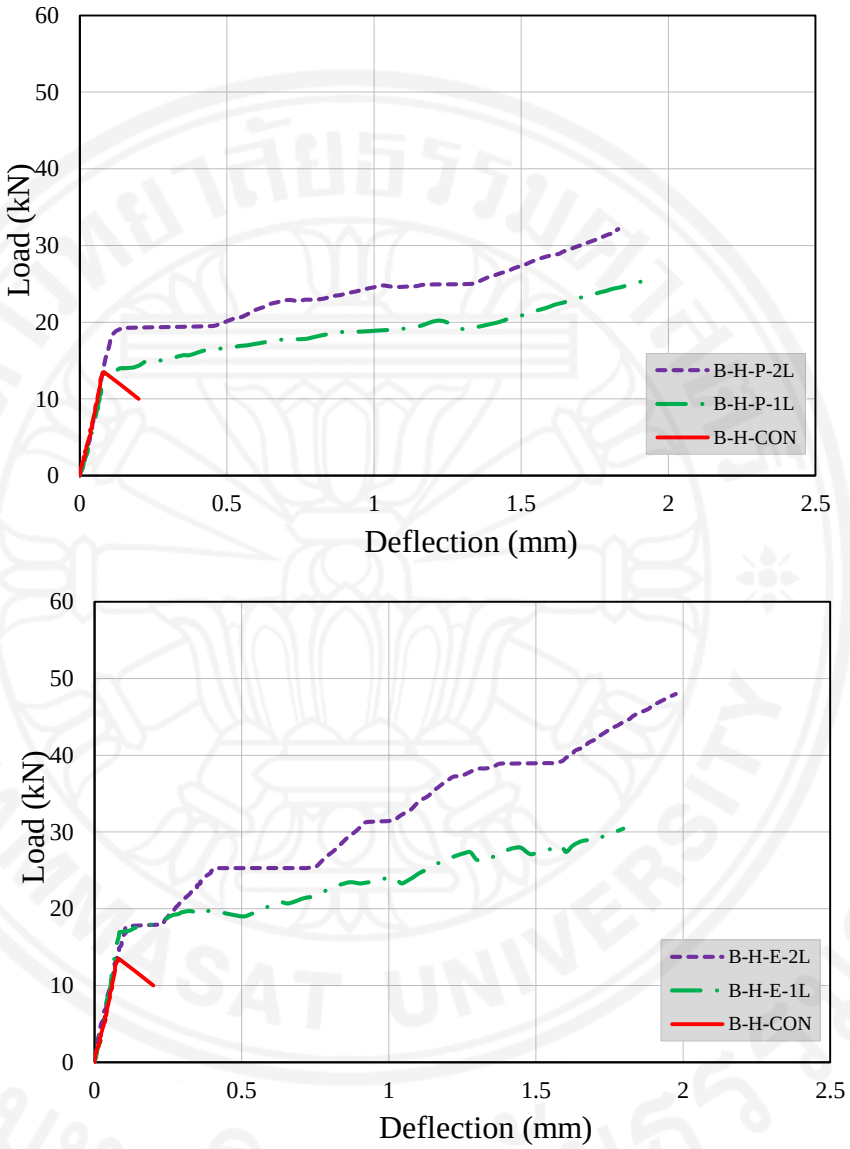

Figure 5.6 Load-mid span deflection curves of beam specimens group C

5.3.1 Effect of test parameters

Fiber thickness, resin matrix and concrete strength were the test parameters in this experimental study. In order to investigate the effect of these parameters, a comparison of ultimate loads is drawn among different beams as shown in Figure 5.7. In this comparison graph, Y-axis represents percentage increase in ultimate load with respect to the control beam in each group. As can be seen that sisal FRP strengthening has significant effect on ultimate load carrying capacity of strengthened

beams. There is found increase in load carrying capacity as the fiber thickness was increased. Both resin matrices are found suitable to bond sisal FRP with concrete, however epoxy resin is found better in performance compared with polyester resin. The efficiency of externally bonded sisal FRPs are found lower for high strength concrete.

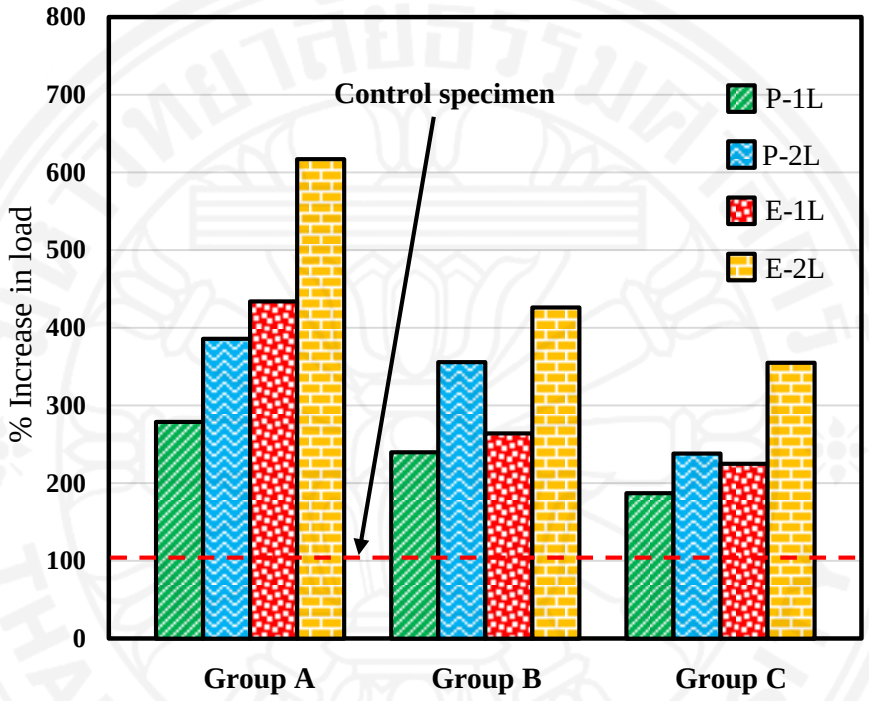

Figure 5.7 Comparison in ultimate load

5.3.2 Failure modes

The typical failure modes of the tested specimen are presented in Figure 5.8. The un-strengthened beams failed suddenly. Whereas sisal FRP strengthened beams failed in a ductile manner. Two types of failures were observed in sisal FRP strengthened beams which were fiber rupture (1 layer of sisal fiber) and de-bonding (2 layers of sisal fiber).

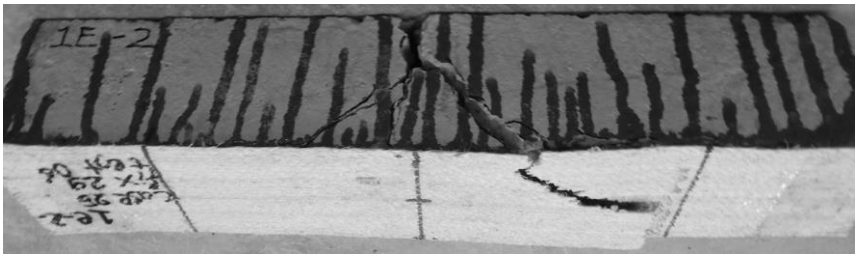

(a) Rupture of FRP

(b) De-bonding of FRP

Figure 5.8 Failure modes of tested beam specimens

5.4 Conclusions

This paper presents experimental results conducted on externally bonded sisal FRP strengthened concrete beams. The test parameters were fiber thickness, resin matrix and concrete strength. Based on results, it can be concluded that sisal FRP is an effective strengthening material. It can be used to enhance the loading capacity of concrete beams. An increase in fiber thickness led to an increase in ultimate load and deflection. Both resin matrices are found suitable to bond sisal FRP with concrete, however epoxy resin is found better in performance compared with polyester resin. The efficiency of sisal FRP to enhance ultimate load is found lower for high strength concrete. The further studies should be carried out to investigate the behavior of reinforced concrete (RC) beams using sisal FRP composites.

Chapter 6

Flexural Strengthening of Reinforced Concrete (RC) Beams using Sisal Fiber Reinforced Polymer (FRP) Composites

6.1 General

This chapter presents an experimental study conducted on the flexural strengthened of reinforced concrete (RC) beams using sisal FRP with different resin matrix. A total of seven RC beams were cast and tested up to failure. Two groups of RC beams were prepared. Group 1 included three RC beams strengthened with externally polyester-bonded sisal FRPs. Group 2 included three RC beams strengthened with epoxy-bonded sisal FRPs. One RC beam was not strengthened and served as control beam for each group. A total length of 1460 mm with a rectangular cross section of 150 mm thick and 180 mm deep were kept the same for all RC beam specimens. The top longitudinal reinforcement consisted of 2DB10, the bottom longitudinal reinforcement consisted of 2RB9. The test parameters included fiber thickness, resin matrix and anchorage system. The load-mid-span-deflection curves of strengthened specimens were plotted against that of control specimen to observe the effect of the investigated parameters on the behavior of RC beams. The failure modes of all tested beams was experimentally observed and discussed in the following sections. Reinforced concrete (RC) beams strengthened by sisal FRP composites may fail by de-bonding of sisal FRP composites from the beam surface. To avoid such failures, an end anchoring system have been proposed and tested to evaluate its performance in preventing the de-bodning of sisal FRP plate from concrete surface.

6.2 Experimental program

6.2.1 Specimen details

The typical reinforcement details and the dimensions of all tested specimens are provided in Figure 6.1. A total length of 1460 mm with a rectangular cross section of 150 mm thick and 180 mm deep were kept the same for all specimens. The top longitudinal reinforcement consisted of 2RB9, the bottom longitudinal reinforcement consisted of 2DB10. The shear reinforcement consisted of 6 mm stirrup bars spaced at 50 mm in the shear zone and at 100 mm and 150 mm in the flexural zone. Clear concrete

cover of 20 mm was provided on all beam faces. One beam was un-strengthened and served as control beam. The other six RC beams were strengthened in flexure with externally bonded sisal FRP composites. The test matrix is briefly provided in Table 6.1.

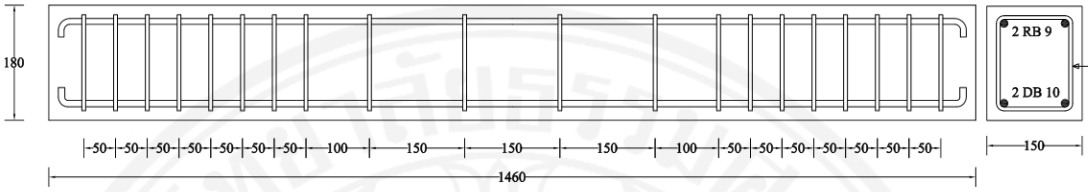

Figure 6.1 Details of RC beam (unit in mm)

Table 6.1 Test matrix

Group	Designation	Fiber thickness (layer)	Anchorage system
Control	Control	-	-
(1) Polyester	P-2L	2	-
	P-2L-AN	2	Epoxy anchor
	P-4L-AN	4	Epoxy anchor
(2) Epoxy	E-2L	2	-
	E-2L-AN	2	Epoxy anchor
	E-4L-AN	4	Epoxy anchor

6.2.2 Material properties

On the testing day (30 days) the compressive strength of concrete was 20 MPa. Mixing proportions is provided in Table 5.2. Sisal fiber was used in this experimental study. Sisal fiber is usually extracted from the leaves of sisal tree, and spun into filaments. It is environmentally friendly and locally available in Thailand. The adhesives used as bonding agent between concrete and hemp FRP were un-saturated polyester and epoxy resin. The tensile strength of sisal FRP composites with polyester and epoxy were approximately 80 MPa and 104MPa, respectively.

Table 6.2 Mix proportions

Compressive strength, MPa	Water kg/ m^3	Cement kg/ m^3	Sand kg/ m^3	Aggregate kg/ m^3
20	213	241	788	1158

6.2.3 Strengthening process

Strengthening process of RC beams using sisal FRP is shown in Figure 6.2 .

(a) Put Sisal fibers under sun light to make it fully dry at least 30 minutes.

(b) Clean the surface of RC beams to remove dust and dirt.

(c) Mix resin and apply on sisal fiber

(d) Apply sisal FRP composite on tension face (bottom) of RC beam

Figure 6.2 Strengthening process

6.2.4 Epoxy anchor with steel plate

The epoxy anchor with steel plate comprised of threaded rod (diameter was 6 mm and length was 75 mm), nut, washer and steel plate. Details of epoxy anchors with steel plates are presented in Figure 6.3 . Sika epoxy prepared as per manufacturer's instructions was filled into the holes. Then threaded rods together with Sika epoxy were inserted into the holes. After the epoxy is perfectly hardened (24 hours), steel plates were installed and nuts were tightened. The installation procedure of epoxy anchor with steel palte is shown in Figure 6.4.

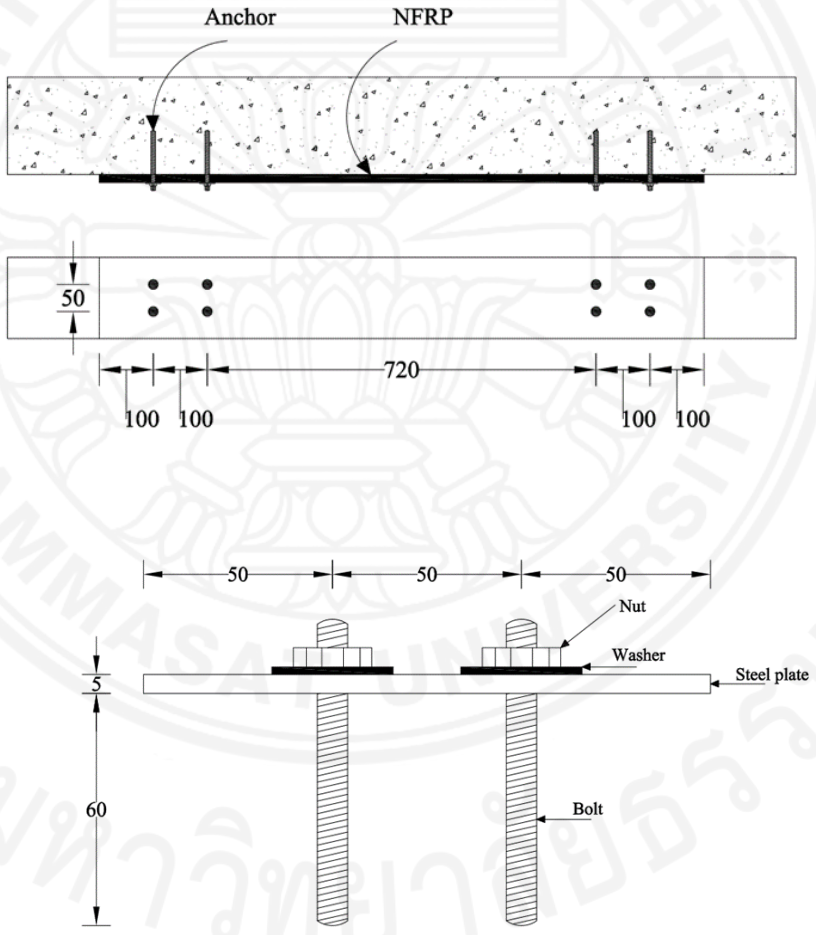

Figure 6.3 Typical anchorage details for sisal FRP strengthened RC beams

(a) The anchor holes were drilled at desired locations

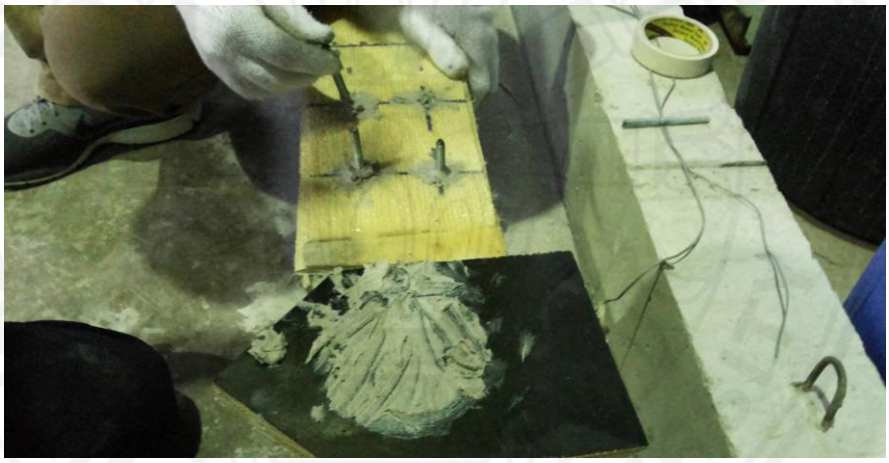

(b) Threaded rods wtted with sika were inserted into the holes

(c) After sika was fully hardened (24 hours), steel plates were placed and nuts were tighted.

Figure 6.4 Epoxy anchorage system preparation

6.2.5 Test setup and instrumentation

All RC beams were designed to fail in flexure, subjected to three-point bending loads in a simply supported arrangement with a shear span of 630 mm giving a shear span-to-depth (a/d) of 3.5. The clear span of each beam was 1260 mm. Load was measured by a calibrated load cell mounted on a hydraulic jack of 500 kN capacity. Deflections were measured at the mid span, quarter span and at two supports of each beam by electronic linear variable differential transducers (LVDT). During the test, the propagation of cracks were carefully observed and recorded by the digital camera. The test set-up is displayed in Figure 6.4.

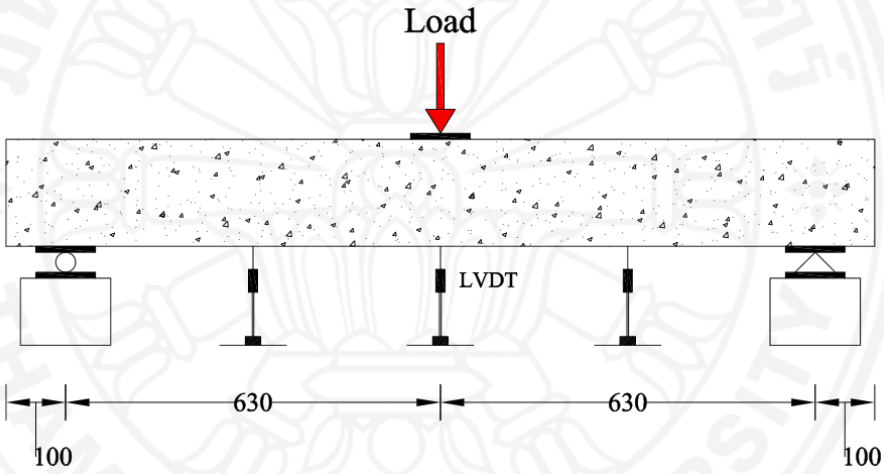

Figure 6.5 Test set up and instrumentation

6.3 Test results and discussions

Table 6.3 Cracking loads

Group	Designation	Cracking Load (Ton)	Increase in cracking load (%)
Control	Control	1.10	-
Polyester	P-2L	1.60	45
	P-2L-AN	1.60	45
	P-4L-AN	1.90	73
Epoxy	E-2L	1.70	54
	E-2L-AN	1.70	54
	E-4L-AN	2.20	100

Experimental load and deflection data were automatically recorded. The cracks and failure modes of the tested specimens were marked and observed during testing until failure. Cracking loads and test results are shown in Table 6.3 and 6.4, respectively.

Table 6.4 Test results of all tested specimens

Designation	Ultimate load (kN)	Load Increase (%)	Mid-span deflection (mm)	Failure mode
Control	47.9	-	31.68	Flexure
P-2L	54.5	14	11.30	De-bonding
P-2L-AN	61.6	29	19.10	Inclined crack
P-4L-AN	65.0	36	20.80	Inclined crack
E-2L	57.1	19	12.53	De-bonding
E-2L-AN	69.2	45	19.71	Inclined crack
E-4L-AN	80.4	68	17.31	Inclined crack

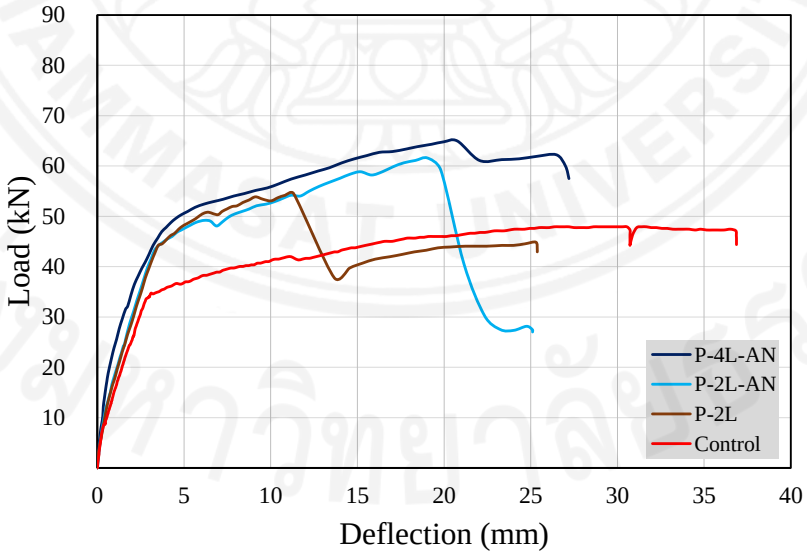

Figure 6.6 Load-mid span deflection of strengthened beams using polyester

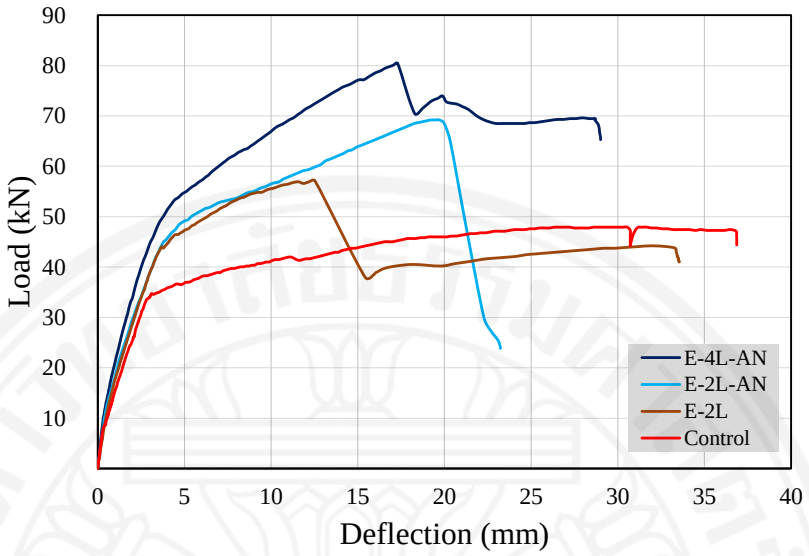

Figure 6.7 Load-mid span deflection of strengthened beams using polyester

The control beam (Control) mainly failed in flexure at the ultimate load of 47.5 kN with a corresponding deflection of 38 mm. Beams P-2L, P-2L-AN and P-4L-AN were strengthened with polyester-bonded sisal FRP composites in the bottom-only scheme. An increase of 12.8% compared to the control beam was obtained for beam P-2L. The beam P-2L-AN failed at the ultimate load of 61.8 kN, which is 30.1% higher than that of the control beam. The Beam P-4L-AN exhibited an ultimate load of 65.8 kN. This led an increase up to 38.5% compared to the control specimen. Beams E-2L, E-2L-AN and E-4L-AN were strengthened with externally epoxy-bonded sisal FRPs, exhibited a load-carrying capacity of 57 kN, 69.3 kN and 80.1 kN with 20%,45.9% and 68.6% increase over that of the control beam, respectively.

6.3.1 Effect of resin system

To study the effect of resin matrix, the results of seven specimens were compared, three of them were strengthened with NFRP using polyester (i.e. P-2L, P-2L-AN, P-4L-AN), three were strengthened with epoxy resin (i.e. E-2L, E-2L-AN, E-4L-AN) and one was the control beam. The load-deflection curves of these specimens are shown in Figure 6.7. A comparison of the normalized load is displayed in Figure 10. As can be seen, the epoxy resin saturated sisal FRP demonstrates a consistently superior performance over polyester resin. This is supposedly due to the high mechanical properties of epoxy resin as compared to the polyester resin. For the polyester resin, the

ultimate load was elevated by 14%, 29% and 36% for the beams P-2L, P-2L-AN and P-4L-AN, respectively, compared with control specimen. Whereas; the beams strengthened with NFRP using epoxy resin (i.e. E-2L, E-2L-AN, E-4L-AN) had the ultimate loads that were 19%, 45% and 68% higher than the control beam, respectively.

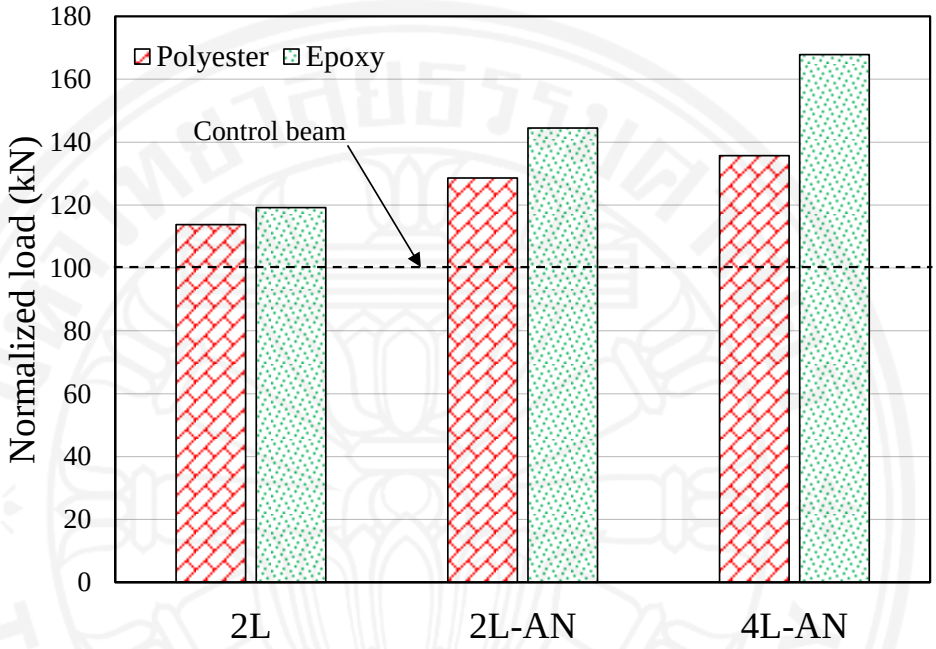

Figure 6.8 Effect of resin matrix

6.3.2 Effectiveness of the end-anchorage system

The proposed end-anchorage system for sisal FRP is found very effective to enhance the bonding between sisal FRP and concrete. The beam specimens P-2L and E-2L (strengthened with two layers of sisal FRP without end anchorage) were failed by de-bonding of sisal FRP from concrete surface in a brittle manner. Whereas; beam specimens P-2L-N and E-2L-AN (strengthened with two layers of sisal FRP without end anchorage) exhibited more ductile behavior than that of beam specimens P-2L and E-2L. The comparison of normalized ultimate load is displayed in Figure 6.8. It can be seen that ultimate load is higher for beam specimens with end anchorage for both polyester and epoxy resin. The beams P-2L-AN and E-2L-AN attained 13% and 21% higher increase in ultimate load compared with beams P-2L and E-2L, respectively. Further, proposed end-anchorage system is also found to be effective to prevent the delamination of fiber when thickness of sisal FRP was increased. In both beam specimens P-4L-AN and E-4L-AN, no de-bonding and pullout of anchors was observed prior to the failure of the beams.

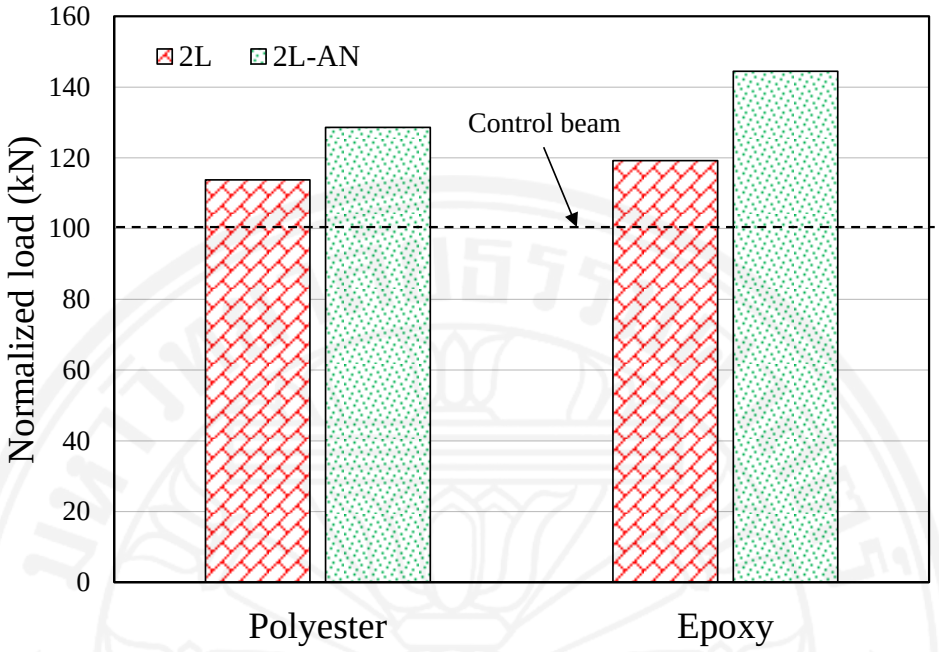

Figure 6.9 Effectiveness of the end-anchorage system

6.3.3 Failure modes

The failure modes of all RC beams are summarized in Table 6.4 and shown in Figure 6.9. The control un-strengthened beam failed in conventional ductile flexure with yielding of the bottom steel bars, followed by slight crushing of the concrete in the compression zone (under loading region) as shown in Figure 6.9(a). The sisal FRP strengthened RC beams without end-anchorage (i.e. P-2L and E-2L) were failed due to sudden and explosive de-bonding of sisal FRP as shown in Figure 6.9(b) and 6.9(c). The delamination of NFRP originated in the center of the beam, and with the further increase in load, it progressed towards ends. Thus, an adequate anchoring system is required for the effective performance of sisal FRP strengthening technique. An end-anchorage system was used to prevent the de-lamination of sisal FRP. The proposed end-anchorage system is found very effective to prevent the delamination of sisal FRP from concrete surface. In all sisal FRP strengthened beams with end-anchoring system (i.e. P-2L-AN, P-4L-AN, E-2L-AN, E-4L-AN), no pullout of anchors and de-bonding of sisal FRP was observed prior to the final failure of the beams. These beams were failed due to the inclined cracks that were formed along the loading and anchoring points as shown in Figure 6.9(d-g).

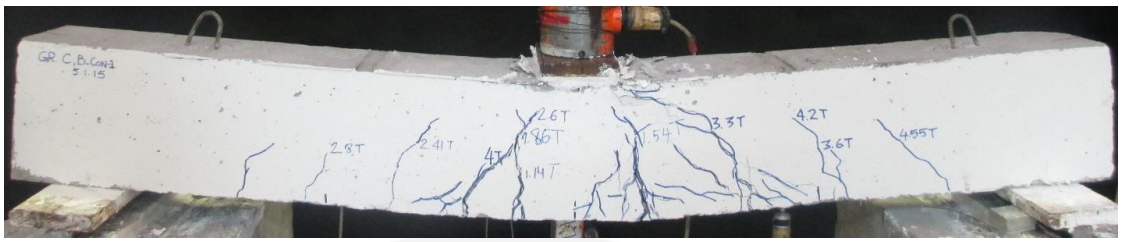

(a) Control beam

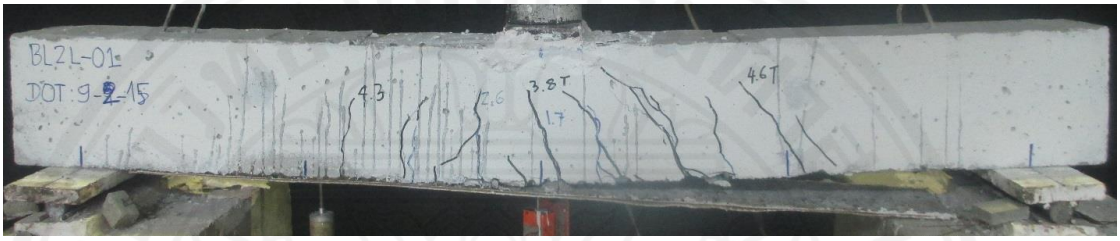

(b) Beam specimen P-2L

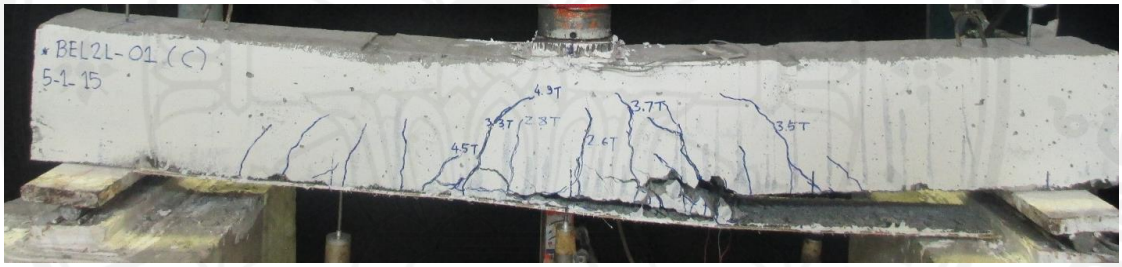

(c) Beam specimen E-2L

(d) Beam specimen P-2L-AN

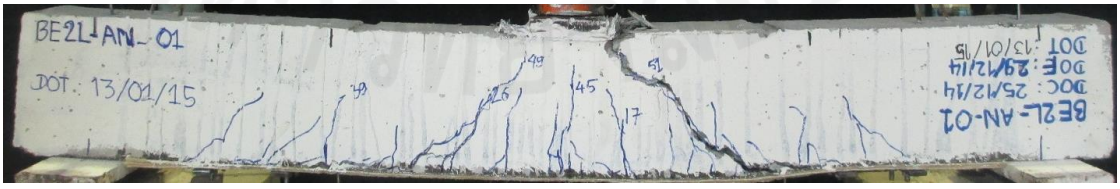

(e) Beam specimen E-2L-AN

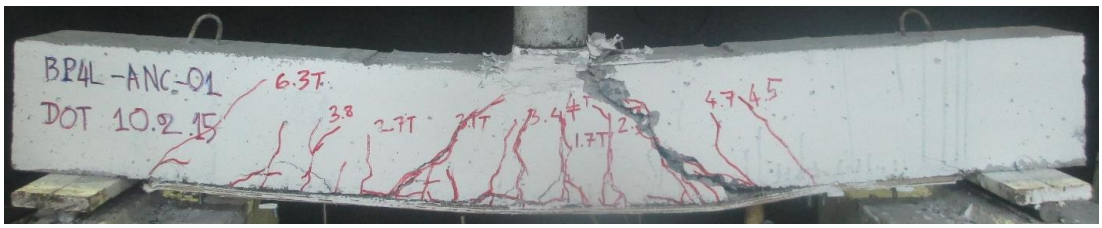

(f) Beam specimen P-4L-AN

(g) Beam specimen E-4L-AN

Figure 6.10 Failure modes of RC beams

6.4 Conclusions

This chapter presents an experimental study conducted on the flexural strengthened of reinforced concrete (RC) beams using sisal FRP with different resin matrix. The test parameters investigated were sisal fiber thickness, resin matrix and anchorage system. Based on the results, the following conclusions were obtained:

1. Significant increase in strength and stiffness of RC beams might be achieved by sisal FRP composites.

2. An increase in fiber thickness led to an increase in ultimate load.

3. Both resin matrices are found effective to bond sisal FRP with concrete, however epoxy resin is found better than un-saturated polyester resin due to better mechanical properties.

4. The proposed epoxy anchors are very effective to prevent the debonding of sisal FRP plate from concrete surface to restore the ductility of sisal FRP strengthened RC beams.

Chapter 7
Flexural Strengthening of Reinforced Concrete (RC) Beams using Hemp FRP Composites

7.1 General

This chapter examines the efficiency of epoxy-bonded hemp fiber reinforced polymer (FRP) composites in flexural strengthening of reinforced concrete (RC) beams. A total of sixteen RC beams were cast and tested up to failure. Two groups of RC beams were prepared. Group 1 included a control RC beam (L-CON) and eight RC beams strengthened with hemp FRPs. A total length of 270 cm with a rectangular cross section of 15 cm thick and 25 cm deep were kept the same for all specimens in group 1. The top longitudinal reinforcement consisted of 2RB9, the bottom longitudinal reinforcement consisted of 2DB10. Group 2 included a control RC beam (H-CON) and six RC beams strengthened with hemp FRPs. A total length of 270 cm with a rectangular cross section of 15 cm thick and 25 cm deep were kept the same for all specimens in group 2. The top longitudinal reinforcement consisted of 2DB10, the bottom longitudinal reinforcement consisted of 2DB16. The test parameters included fiber thickness, strengthening configuration, anchorage system and internal reinforcement. The load-mid-span-deflection curves of strengthened specimens were plotted against that of control specimen to observe the effect of the investigated parameters on the behavior of RC beams. The failure modes of all tested beams was experimentally observed and discussed in the following sections.

7.2 Experimental program

Reinforcing steel bars which were used as internal reinforcement in this research works was also obtained from Rung Sin Co. Ltd., Thailand. The mechanical properties of all reinforcing steel bars using in this research work were provided in Section 6.2.4.

7.2.1 Specimen details and test matrix of specimens group 1

The typical reinforcement details and the dimensions of all tested specimens in group 1 are provided in Figure 7.1 A total length of 270 cm with a rectangular cross section of 15 cm thick and 25 cm deep were kept the same for all specimens. The top

longitudinal reinforcement consisted of 2RB9, the bottom longitudinal reinforcement consisted of 2DB10. The shear reinforcement consisted of 6 mm stirrup bars spaced at 50 mm in the shear zone and at 100 mm in the flexural zone. Clear concrete cover of 20 mm was provided on all beam faces. One beam was un-strengthened and served as control beam. The other eight RC beams were strengthened in flexure with externally bonded hemp FRP composites. The test matrix is briefly provided in Table 7.1.

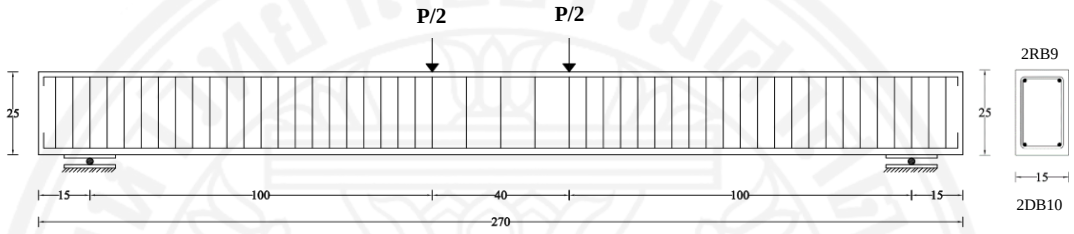

Figure 7.1 Details of test specimen group 1 (unit in cm)

Table 7.1 Test Matrix of all specimens in group 1

Designation	Strengthening scheme	Fiber thickness (layer)	Anchorage system
L-CON	Control	-	-
L-B-1L	Bottom only	1	-
L-B-2L	Bottom only	2	-
L-B-3L	Bottom only	3	-
L-B-3L-EA	Bottom only	3	Epoxy anchor
L-B-3L-UA	Bottom only	3	U-end anchor
L-U-1L	U-wrap	1	-
L-U-2L	U-wrap	2	-
L-U-3L	U-wrap	3	-

7.2.2 Specimen details and test matrix of specimens group 2

The typical reinforcement details and the dimensions of all tested specimens in group 2 are provided in Figure 7.2. A total length of 270 cm with a rectangular cross section of 15 cm thick and 25 cm deep were kept the same for all specimens. The top longitudinal reinforcement consisted of 2DB10, the bottom longitudinal reinforcement consisted of 2DB16. The shear reinforcement consisted of 6 mm stirrup bars spaced at 50 mm in the shear zone and at 100 mm in the flexural zone. Clear concrete cover of 20

mm was provided on all beam faces. One beam was un-strengthened and served as control beam. The other eight RC beams were strengthened in flexure with externally bonded hemp FRP composites. The test matrix is briefly in Table 7.2.

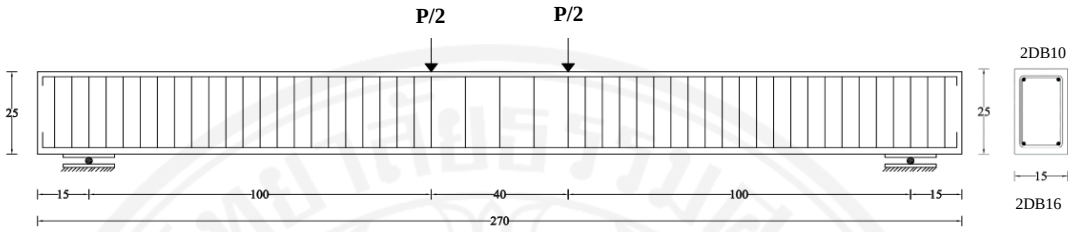

Figure 7.2 Details of test specimen group 2 (unit in cm)

Table 7.2 Test Matrix of all specimens in group 2

Designation	Strengthening scheme	Fiber thickness (layer)	Anchorage system
H-CON	Control	-	-
H-B-2L	Bottom only	2	-
H-B-3L	Bottom only	3	-
H-B-3L-EA	Bottom only	3	Epoxy anchor
H-B-3L-UA	Bottom only	3	U-end anchor
H-U-2L	U-wrap	2	-
H-U-3L	U-wrap	3	-

7.2.3 Material properties

On the testing day (30 days) the compressive strength of concrete was 24 MPa. Mix proportions are given in Table 7.3. Hemp fiber was used in this experimental study. Hemp fiber is usually extracted from the leaves of hemp tree, and spun into filaments. It is environmentally friendly and locally available in Thailand. The tensile strength of hemp FRP composites was approximately 156 MPa. The adhesive used as bonding agent between concrete and hemp FRP was epoxy resin.

7.2.4 Test setup and instrumentation

All RC beams were designed to fail in flexure, subjected to four-point bending loads in a simply supported arrangement. The clear span of each beam was 240 cm. Load was measured by a calibrated load cell mounted on a hydraulic jack of 500 kN

capacity. Deflections were measured at the mid span, quarter span and at two supports of each beam by electronic linear variable differential transducers (LVDT). During the test, the propagation of cracks were carefully observed and recorded by the digital camera. The test set-up is displayed in Figure 7.3.

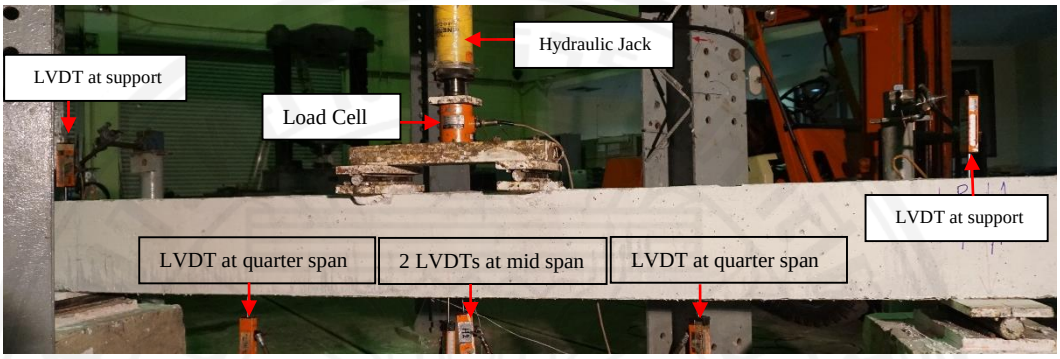

Figure 7.3 Test setup

7.3 Test results and discussions

7.3.1 Specimens group 1

Table 7.3 Experimental results of all tested specimens in group 1

Specimen	Peak load (kN)	Load increase (%)	Mid-span deflection (mm)	Failure mode
L-CON	38.92	-	60	Flexure, steel bars yielding
L-B-1L	46.71	20.0	21.56	Steel bars yielding and FRP rupture
L-B-2L	56.21	44.4	24.66	Steel bars yielding and FRP rupture
L-B-3L	68.44	75.8	22.45	FRP de-bonding
L-B-3L-EA	65.19	67.5	25.78	FRP rupture
L-B-3L-UA	66.72	71.4	25.87	FRP rupture
L-U-1L	57.93	48.8	20.56	Steel bars yielding and FRP rupture
L-U-2L	83.91	115.6	24.12	Steel bars yielding and FRP rupture
L-U-3L	112.8	189.8	28.35	Steel bars yielding and FRP rupture

7.3.1.1 Test results

Group 1 consisted of nine specimens which were tested in two-point loading until failure. The effect of fiber thickness, strengthening configuration and end-anchorage

system can be observed in this group by comparing with the un-strengthened specimen. Experimental load and deflection data were automatically recorded. The cracks and failure modes of the tested specimens were marked and observed during testing until failure. Test results of all experimental specimens are discussed in Table 7.3. and the load-deflection responses of strengthened beams were plotted against that of control specimen to observe the effect of hemp FRP composites on RC beams. The experimental results of tested specimens are presented in Table 7.3.

The control beam (L-CON) mainly failed in flexure at the ultimate load of 38.92 kN with a corresponding deflection of 60 mm. Beams L-B-1L, L-B-2L and L-B-3L were strengthened with hemp FRP in the bottom-only scheme. An increase of 20% compared to the control beam was obtained for beam L-B-1L. The beam L-B-2L failed at the ultimate load of 56.21 kN, which is 44% higher than that of the control beam. L-B-3L exhibits an increase in peak load of 68.44 kN, which is higher than control specimen about 76%. Load-mid span deflection curves of strengthened beams in bottom-only together with control specimen are presented in Figure 7.4.

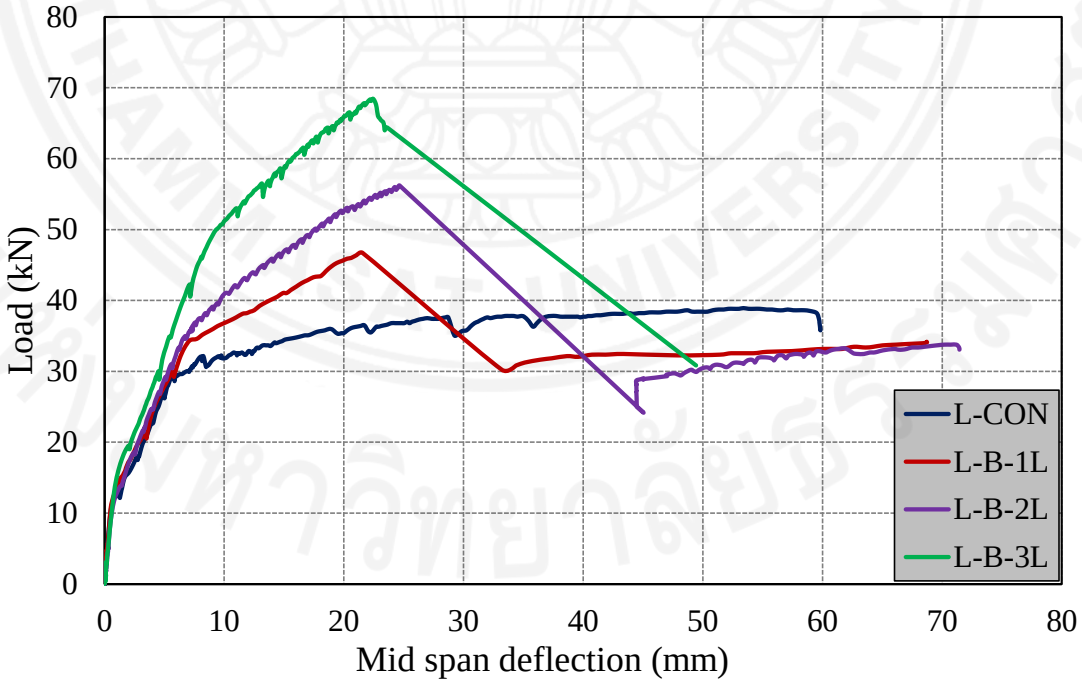

Figure 7.4 Load-mid span deflection curves of strengthened beams in bottom-only configuration

Hemp FRP strengthened beams with end-anchoring system (i.e. L-B-3L-EA, L-B-3L-UA) failed at the peak loads of 65.19 kN and 66.72 kN, which were 67.5% and 71% higher than that control beam, respectively. Load-mid span deflection curves of L-B-3L-EA and L-B-3L-UA are presented in Figure 7.5, respectively.

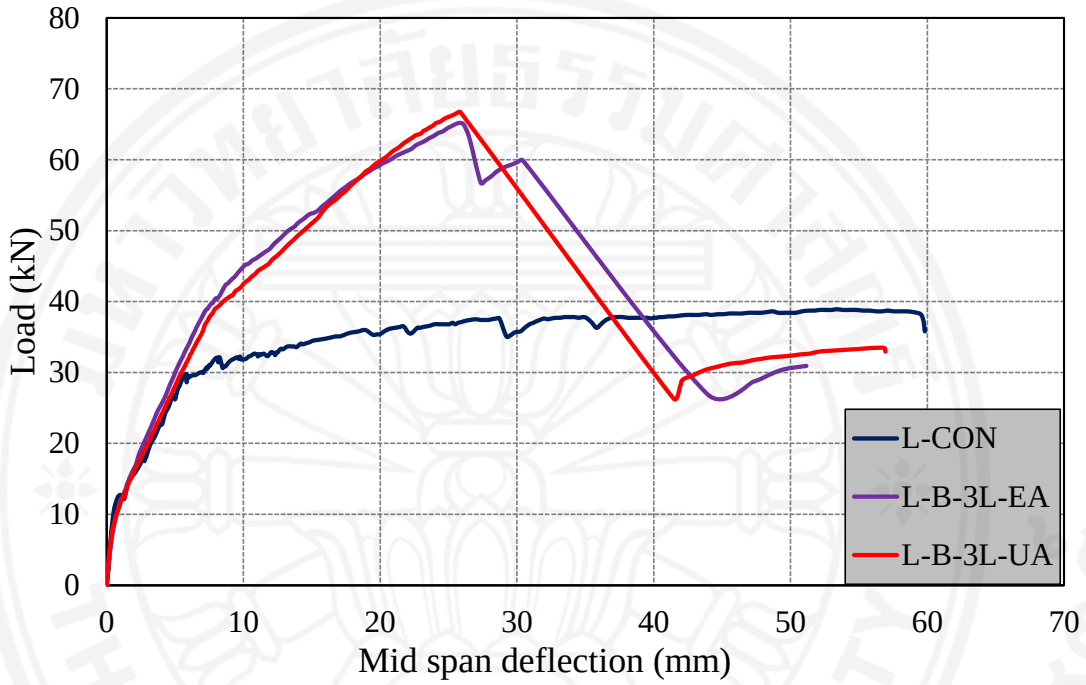

Figure 7.5 Load-mid span deflection curves of strengthened beams with end-anching systems

Beams L-U-1L, L-U-2L and L-U-3L were strengthened in the U-wrapped scheme, exhibited a load-carrying capacity of 57.93 kN, 83.91 kN and 112.8 kN with 49%,116% and 190% increase over that of the control beam, respectively. Load-mid span deflection curves of L-U-1L, L-U-2L and L-U-3L are shown in Figure 7.6 , respectively.

7.3.1.2 Effect of fiber thickness

The effects of hemp fiber thickness on the ultimate strength of hemp FRP strengthened RC beams are shown in Figure 7.12 and 7.13. As it can be seen, 20% , 44% and 75.8% increases in ultimate load were observed for L-B-1L, L-B-2L and L-B-3L, respectively. Whereas, 49%, 116% and 190% increases in loading capacity were recorded for L-U-1L, L-U-2L and L-U-3L, respectively. Based on results it can be

concluded that, an increase in fiber thickness led to increase in ultimate load of hemp FRP strengthened beam.

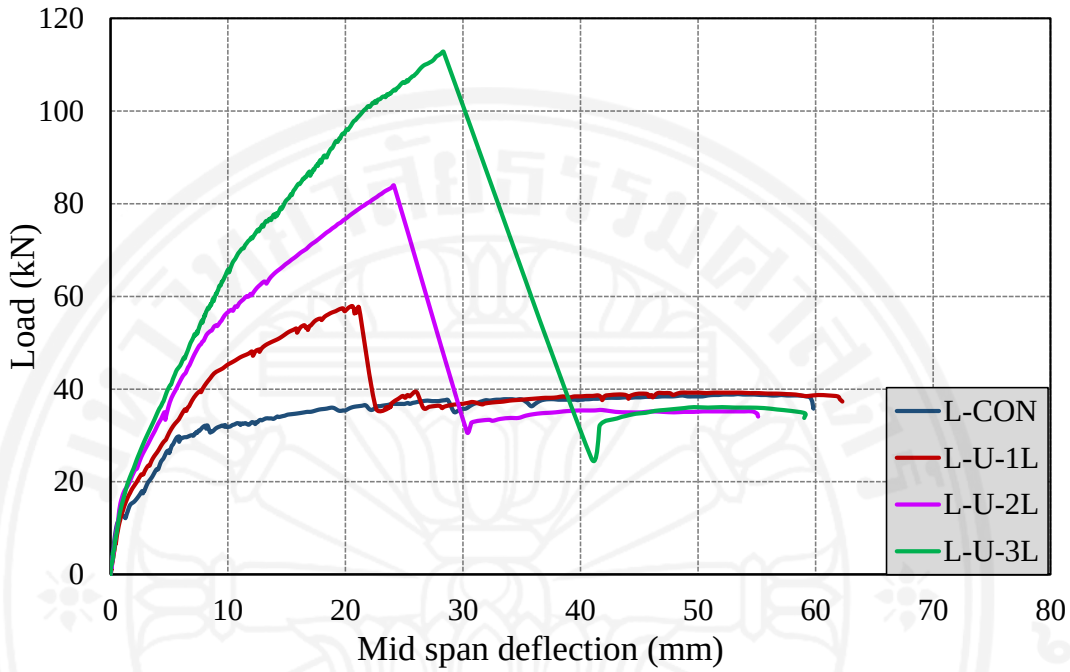

Figure 7.6 Load-mid span deflection curves of strengthened beams in U-wrap configuration

7.3.1.3 Effect of strengthening configuration

To study the effect of strengthening configuration, the results of several specimens were compared (i.e. L-B-1L compared with L-U-1L, L-B-2L compared with L-U-2L). It can be seen that, beam L-U-1L showed an increase of strength capacity higher than L-B-1L. Whereas, beam L-U-2L obtained an increase in the ultimate load greater than L-B-2L. Due to higher FRP reinforcement ratio, U-wrap scheme is found more effective to increase the loading capacity than bottom-only sceme. A comparison of the normalized load is displayed in Figure 7.7.

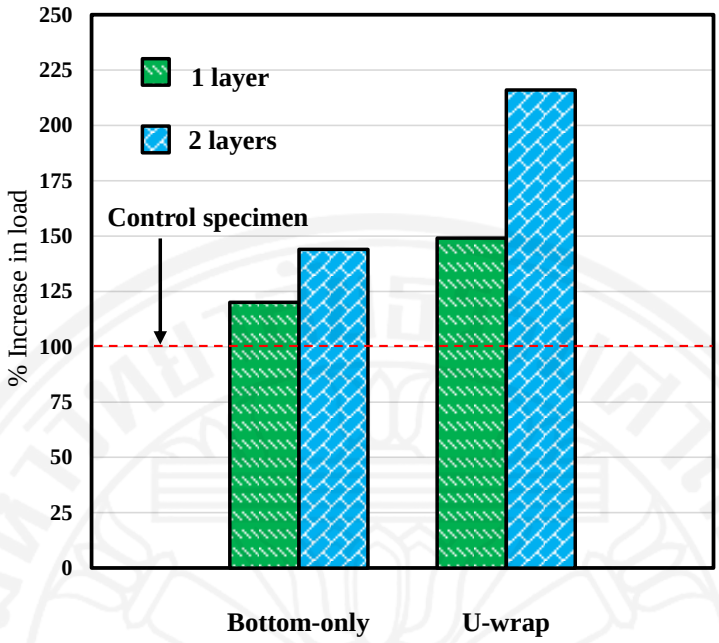

Figure 7.7 comparison in ultimate load

7.3.1.4 Effectiveness of end-anchorage system

The proposed end-anchorage system for hemp FRP is found very effective to enhance the bonding between hemp FRP and concrete. The beam specimens L-B-3L (strengthened with three layers of hemp FRP in bottom-only scheme without end anchorage) were failed by de-bonding of hemp FRP from concrete surface in a brittle manner. Whereas, beam specimens L-B-3L-EA and L-B-3L-UA (strengthened with three layers of hemp FRP using end-epoxy anchorage and U-end hemp anchorage systems) exhibited more ductile behavior than that of beam specimen B-L-3L. No de-bonding and pullout of anchors was observed prior to the failure of the beams. Further, proposed end-anchorage systems are also found to be effective to prevent the delamination of fiber when thickness of hemp FRP was increased.

7.3.1.5 Failure modes

The first visible flexural crack of control beam occoured at a load of 12 kN. It failed in converntional ductile flexure with yielding of the bottom steel bars at the load of 38.92 kN. The hemp FRP strengthened beams in bottom-only scheme (i.e. L-B-1L and L-B-2L) failed due to rupture of hemp FRP composites as shown in Figure 7.8(a). Whereas L-B-3L failed due to sudden and explosive de-bonding of hemp FRP composite as shown in Figure 7.8(b). The delamination of hemp FRP originated in the center of the

beam, and with the further increase in load, it progressed towards ends. Thus, an adequate anchoring system is required for the effective performance of hemp FRP strengthening technique. End-anchorage systems (i.e. epoxy anchor and U-end anchor) were used to prevent the de-lamination of hemp FRP. The proposed end-anchorage systems are found very effective to prevent the delamination of hemp FRP from concrete surface. In all hemp FRP strengthened beams with end-anchoring system (i.e. L-B-3L-EA, L-B-3L-UA), no pullout of anchors and de-bonding of hemp FRP were observed prior to the final failure of the beams. The hemp FRP strengthened beams in U-wrap scheme (i.e. L-U-1L, L-U-2L and L-U-3L) failed due to rupture of hemp FRP composites as shown in Figure 7.8(e).

(a)

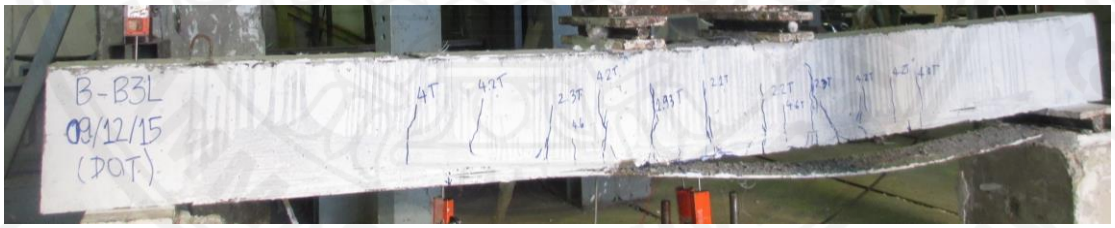

(b)

(c)

(d)

(e)

Figure 7.8 Failure modes of tested strengthened RC beams

7.3.2 Specimens group 2

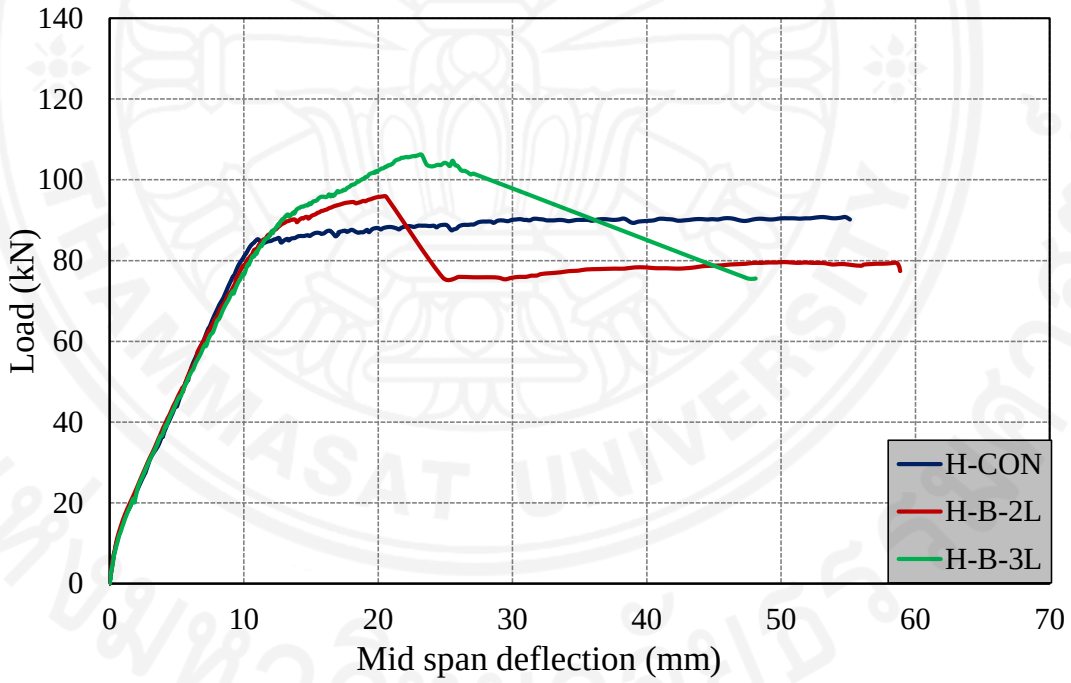

Figure 7.9 Load-mid span deflection curves of tested beams in bottom-only configuration

The control beam (H-CON) mainly failed in flexure at the ultimate load of 90.78 kN with a corresponding deflection of 58 mm. Beams H-B-2L and H-B-3L were strengthened with hemp FRP in the bottom-only scheme. An increase of 5.6% compared to the control beam was obtained for beam H-B-1L. The beam H-B-2L failed at the ultimate load of 106.3 kN, which is 17.1% higher than that of the control beam. Load-

mid span deflection curves of strengthened beams in bottom-only scheme are presented in Figure 7.9.

Hemp FRP strengthened beams with end-anchoring system (i.e. H-B-3L-EA, H-B-3L-UA) failed at the peak loads of 108.6 kN and 108.9 kN, which were 19.6% and 20% higher than that control beam, respectively. Load-mid span deflection curves of H-B-3L-MA and H-B-3L-UA are presented in Figure 7.10 .

Beams H-U-2L and H-U-3L were strengthened in the U-wrapped scheme, exhibited a load-carrying capacity of 120.3 kN and 132.2 kN with 32.5% and 44.5% increase over that of the control beam, respectively. Load-mid span deflection curves of H-U-2L and H-U-3L are shown in Figure 7.11.

Table 7.4 Results of tested beam specimens in group 2

Specimen	Ultimate load (kN)	Load increase (%)	Failure mode
H-CON	90.78	-	Flexure, steel bars yielding
H-B-2L	95.90	5.6	Steel bars yielding and FRP rupture
H-B-3L	106.3	17.1	FRP debonding
H-B-3L-EA	108.6	19.6	FRP rupture
H-B-3L-UA	108.9	20.0	FRP rupture
H-U-2L	120.3	32.5	Steel bars yielding and FRP rupture
H-U-3L	131.2	44.5	Steel bars yielding and FRP rupture

7.3.2.1 Effect of test parameters

Fiber thickness, strengthening configuration and anchorage system were the test parameters in this experimental study. In order to investigate the effect of these parameters, a comparison of ultimate loads is drawn among different beams as shown in Figure 7.12. In this comparison graph, Y-axis is representing percentage increase in ultimate load with respect to the control beam in each group. As can be seen that hemp FRP strengthening has significant effect on ultimate load carrying capacity of strengthened beams. There is found increase in load carrying capacity as the fiber thickness was increased. U-wrap scheme is found more effective than bottom-only scheme. Anchorage systems helped to prevent de-bonding of hemp FRP and restore some of losing ductility.

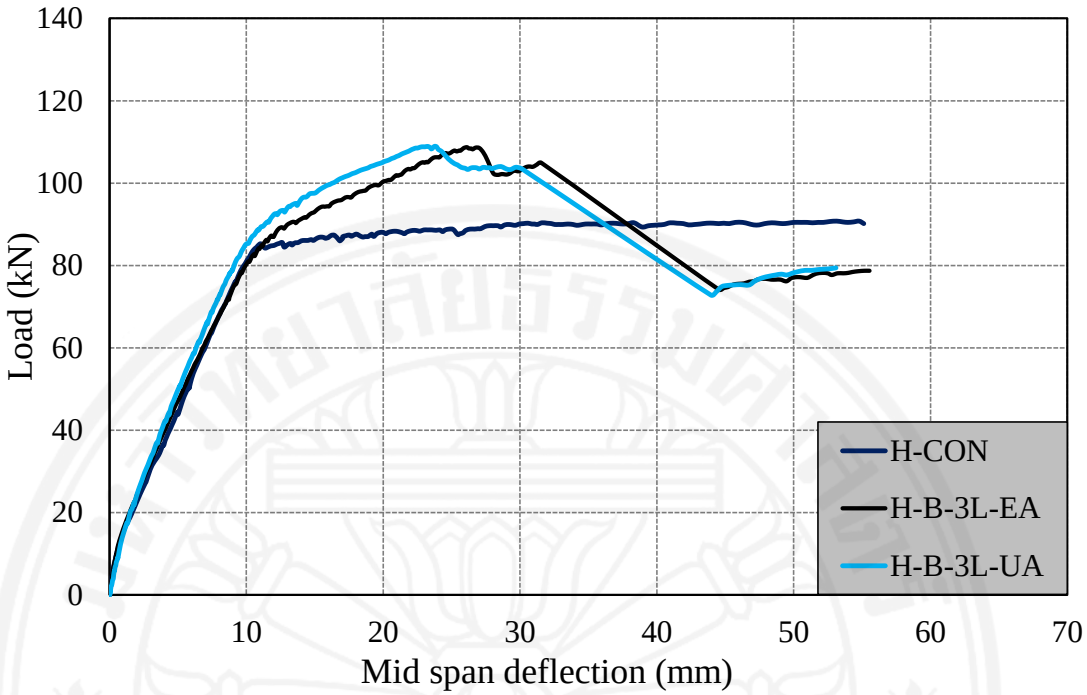

Figure 7.10 Load-mid span deflection curves of tested beams with anchorage systems

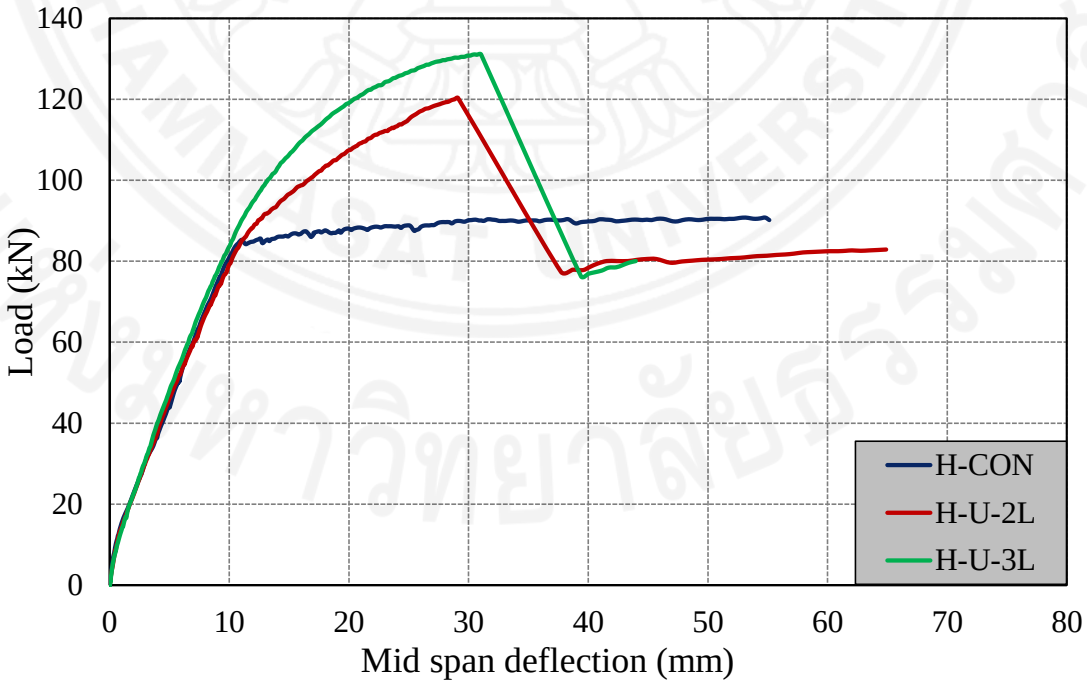

Figure 7.11 Load-mid span deflection curves of tested beams in U-wrap configuration

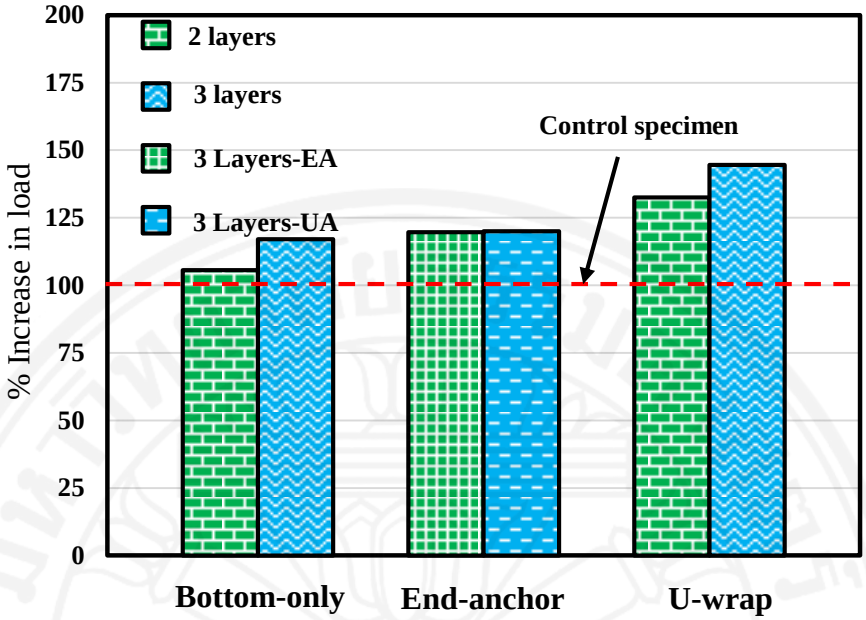

Figure 7.12 Comparison in ultimate load

7.3.2.2 Failure modes

Control beam (H-CON) failed in converntional ductile flexure with yielding of the bottom steel bars at the load of 90.78 kN. The hemp FRP strengthened beams in bottom-only scheme (i.e. H-B-2L) failed due to rupture of hemp FRP composites as shown in Figure 7.13(a). Whereas H-B-3L failed due to sudden and explosive de-bonding of hemp FRP composite as shown in Figure 7.13(b). The delamination of hemp FRP originated in the center of the beam, and with the further increase in load, it progressed towards ends. Thus, an adequate anchoring system is required for the effective performance of hemp FRP strengthening technique. Epoxy anchor and U-end anchor were used to prevent the de-lamination of hemp FRP as shown in Figure 7.13(c-d) . The proposed end-anchorage systems are found very effective to prevent the delamination of hemp FRP from concrete surface. In all hemp FRP strengthened beams with end-anchoring system (i.e. H-B-3L-EA, H-B-3L-UA), no pullout of anchors and de-bonding of hemp FRP were observed prior to the final failure of the beams. The hemp FRP strengthened beams in U-wrap scheme (i.e. H-U-2L and H-U-3L) failed due to rupture of hemp FRP composites as shown in Figure 7.13(e-f).

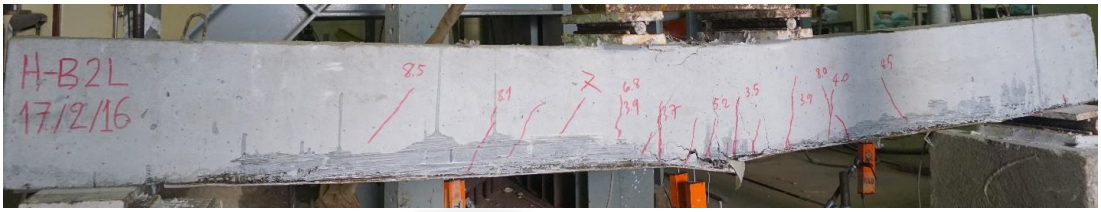

(a)

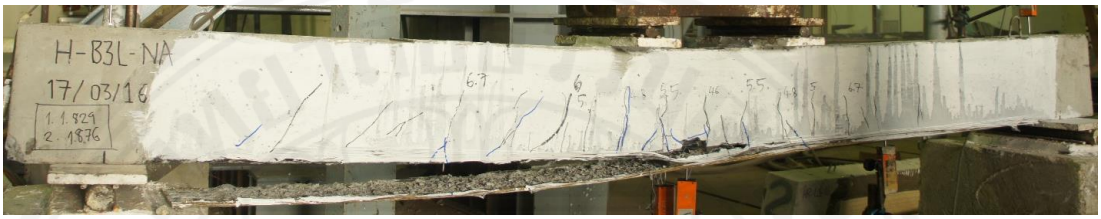

(b)

(c)

(d)

(e)

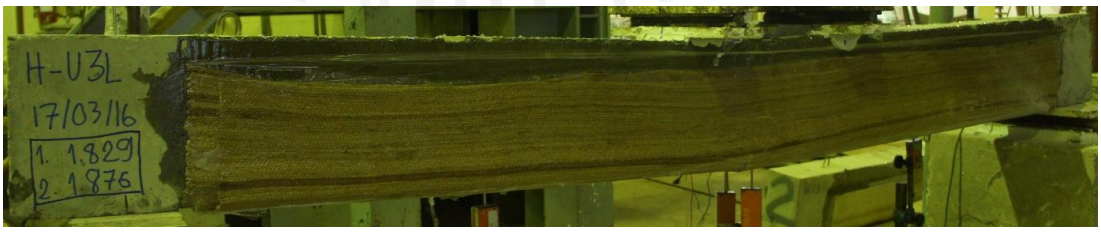

(f)

Figure 7.13 Failure modes of tested strengthened RC beams in group 2

7.4 Conclusions

This chapter presents an experimental study conducted on the flexural strengthened of reinforced concrete (RC) beams using hemp FRP composites. The test parameters investigated were hemp fiber thickness, strengthening configuration and anchorage system. Based on the results, the following conclusions were obtained:

1. Significant increase in strength and stiffness of RC beams might be achieved by hemp FRP composites.

2. An increase in fiber thickness led to an increase in ultimate load.

3. Both strengthening configurations are found effective. However U-wrap scheme is better due to higher FRP reinforcement ratio.

4. The proposed epoxy anchors and U-end (hemp) anchor are very effective to prevent the debonding of hemp FRP plate from concrete surface to restore the ductility of sisal FRP strengthened RC beams.

5. Strengthened beams in the low (internal) reinforcement group were increased in ultimate load higher than strengthened beams in the high reinforcement group.

Chapter 8
Finite Element Modeling of Reinforced Concrete (RC) Beams Strengthened using Hemp FRP Composites

8.1 General

This chapter examines the finite element analysis carried out on reinforced concrete (RC) beams strengthened in flexure using hemp fiber reinforced polymer (FRP) composites. The analysis parameters consisted of hemp FRP thickness (1 layer, 2 layers, and 3 layers), strengthening configurations (bottom and U-wrapped scheme) and internal reinforcement (low and high reinforcement ratio). The ultimate loading capacity of reinforced concrete (RC) beam is effectively enhanced by bonding hemp FRP composites externally to the tension face of the beam. The load-mid span response of strengthened reinforced concrete deep beams were analytically investigated by using a finite elemet (FE) software. Comparisons are made between analytical and experimental results considering the material constitutive models and behavior mechanisms of FE software to assess its accuracy in predicting the actual response of these specimens. The experimental results of strengthened RC deep beams which were tested and presented in chapter 6 were used here to compare with those of the finite element program VecTor2. VecTor2 is a nonlinear finite element (FE) software which has been developed at the University of Toronto. FE program VecTor2 was used for the modeling and analysis of RC beams externally strengthened using hemp FRP composites.

8.2 The VecTor2 program

VecTor2 is a nonlinear finite element program based on Disturbed Stress Field Model (DSFM) which is a refinement of Modified Compression Field theory (MCFT) [30, 31]. It considers smeared rotating crack concept which is based on the displacement-based analytical approach [32]. VecTor2 uses a fine mesh of low-powered elements for its models that are computationally efficient and numerically stable. These elements include a three-node triangle, a four-node rectangular and a four-node quadrilateral element for modeling concrete with smeared reinforcement. For discrete reinforcement, a two-node truss-bar element is used and for modeling bond-slip mechanisms, a two-node link and a four-node contact element is used [33]. The finite

element model is constructed in FormWorks, a pre-processor software that generate input files for VecTor2, and the results are visualized in Augustus program which is a post-processor.

8.3 Modeling of concrete and reinforcement

The finite element mesh of the reinforced concrete (RC) beam is illustrated in Figure 8.1. Plane stress rectangular elements of 25 mm by 25 mm were used for modeling reinforced concrete.

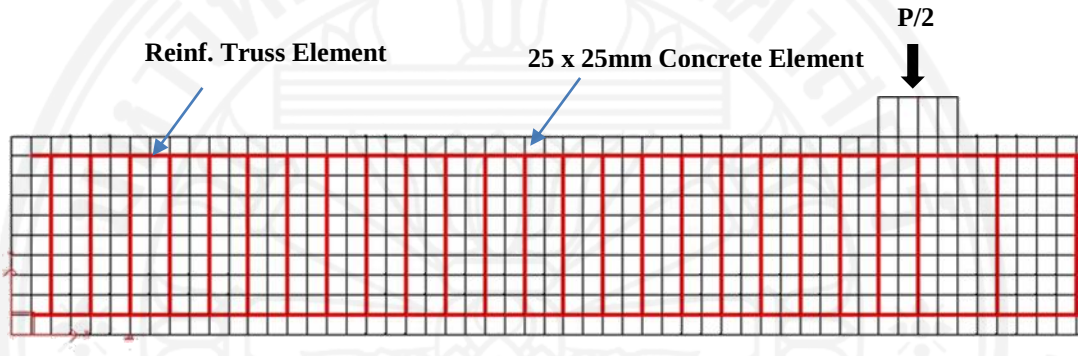

Figure 8.1 Finite element mesh of the RC beam

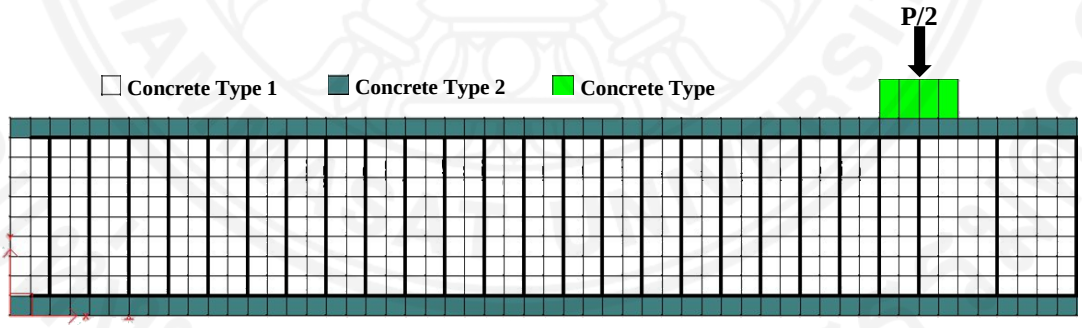

Figure 8.3 Concrete element type

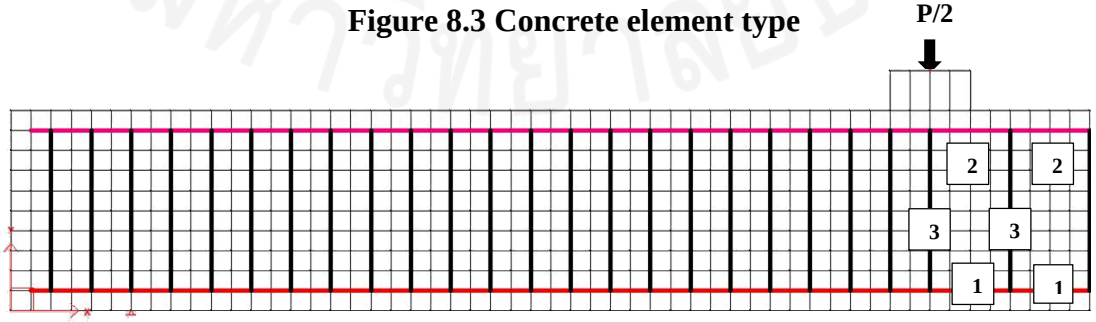

Figure 8.4 Assignment of reinforcement material

Table 8.1 Reinforcement element type for beam specimens group 1

Reinforcement Type	Location	Size
1	Bottom longitudinal reinforcement	DB10
2	Top longitudinal reinforcement	RB9
3	Shear reinforcement	RB6

Table 8.2 Reinforcement element type for beam specimens group 2

Reinforcement Type	Location	Size
1	Bottom longitudinal reinforcement	DB16
2	Top longitudinal reinforcement	DB10
3	Shear reinforcement	RB6

The FormWorks model of reinforced concrete deep beam is illustrated in Table 8.3. The descriptions of how to model the concrete materials and reinforcement component in FormWorks are detailed in VecTor2 and FormWorks User's Manual [33]

8.4 Concrete and reinforcement analytical models

The selected material and behavioral models for concrete elements, reinforcement elements are given in Figure 8.5. The details of all material and behavioral models mentioned below are available in Vector2 and FormWorks User's Manual [33].

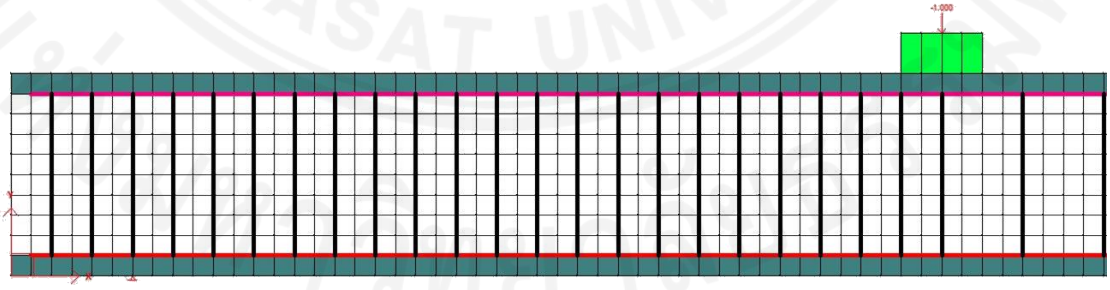

Figure 8.5 FormWorks model of reinforced concrete beam

Table 8.3 Analytical models used in the FE analyses

Material Properties	Analytical Model
Concrete Model	
Concrete compression pre-peak response	Hognestad (Parabola)
Concrete Compression post-peak response	Modified Park-Kent
Concrete Compression Softening Model	Vecchio 1992-A (e1/e2-Form)
Concrete Tension Stiffening Model	Modified Bentz 2003
Concrete Tension Softening Model	Linear
Concrete Confined Strength	Kupfer/Richart
Concrete Lateral Expansion	Variable-Kupfer
Concrete Cracking Criterion	Mohr-Coulomb (Stress)
Concrete Crack Stress Calculation	Basic (DSFM/MCFT)
Concrete Crack Width Check	Agg/2.5 Max Crack Width
Concrete Crack Slip Calculation	Walraven (Monotonic)
Concrete creep and relaxation	Not available
Concrete Hysteretic Response	Linear w/Plastic Offsets
Reinforcement Models	
Reinforcement Hysteretic response	Bauschinger Effect (Seckin)
Reinforcement Dowel action	Tassios (Crack Slip)
Reinforcement Buckling	Refined Dhakal-Maekawa
Bond Models	
Concrete Bond	Eligehausen Model

8.5 Comparison of analytical and experimental results

8.5.1 Specimens group 1

A comparison between experimental and analytical values for selected specimens are summarized and compared in Table 8.4. It can be seen that the results obtained from the VecTor2 were in good accordance with the experimental results. The crack patterns of RC beams observed during testing and the predicted finite lement results are compared and discussed in the following sections.

Table 8.4 Summary and comparison of experimental and analytical results of beam specimens group 1

Specimen	Ultimate load (kN)		Analytical/Experimental
	Experimental	Analytical	
L-CON	38.92	39.1	1.00
L-B-1L	46.71	48.8	1.04
L-B-2L	56.21	55.5	0.99
L-B-3L	68.44	71.0	1.04
L-U-1L	57.93	56.6	0.98
L-U-2L	83.91	84.5	1.01
L-U-3L	112.8	109.5	0.97

The finite element models can predict the behavior of un-strengthened and strengthened RC beams. This finite element program is also capable of predicting cracks at every load steps.

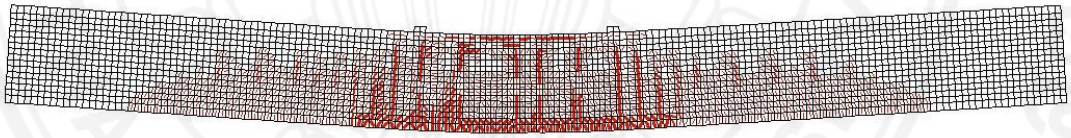

(a) Control beam

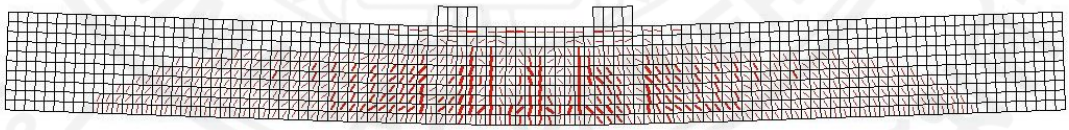

(b) L-B-1L

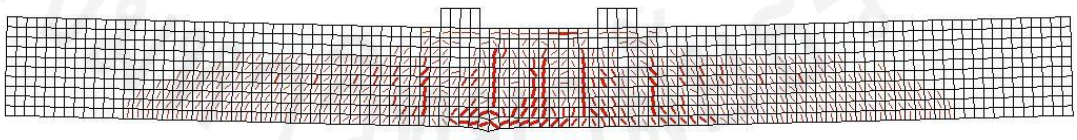

(c) L-B-2L

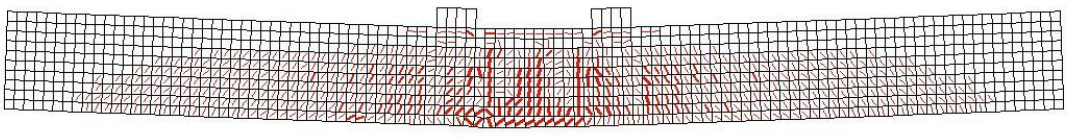

(d) L-B-3L

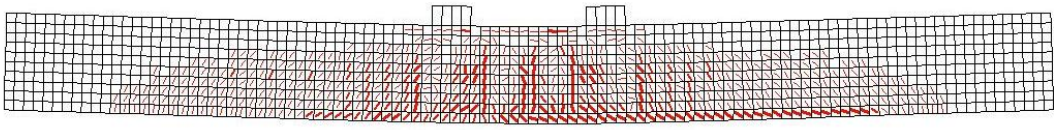

(e) L-U-1L

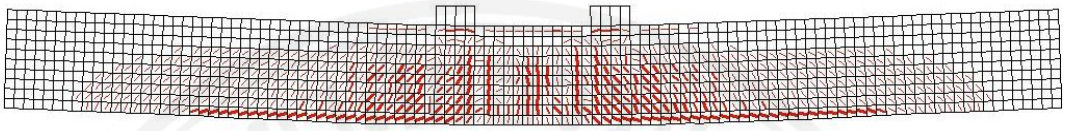

(f) L-U-2L

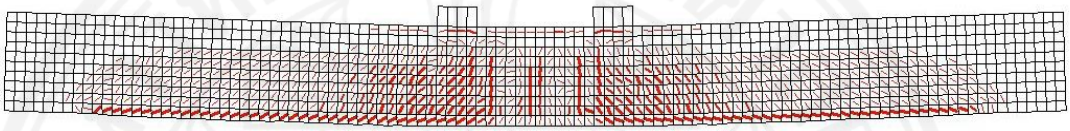

(g) L-U-3L

Figure 8.6 Crack patterns of RC beams group 1

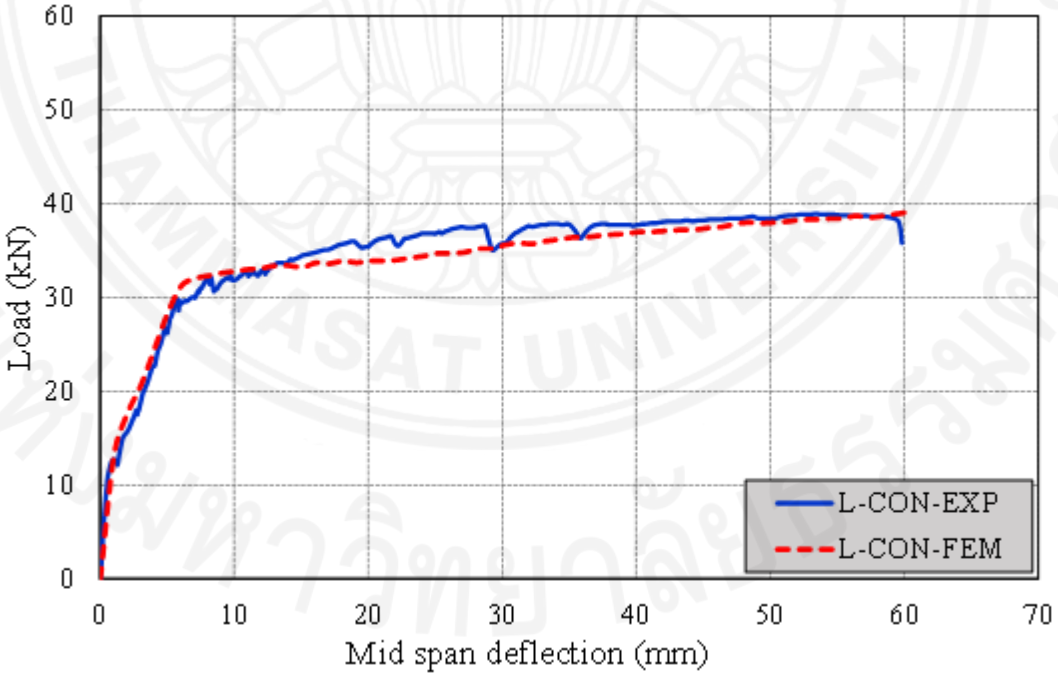

(a) Control beam

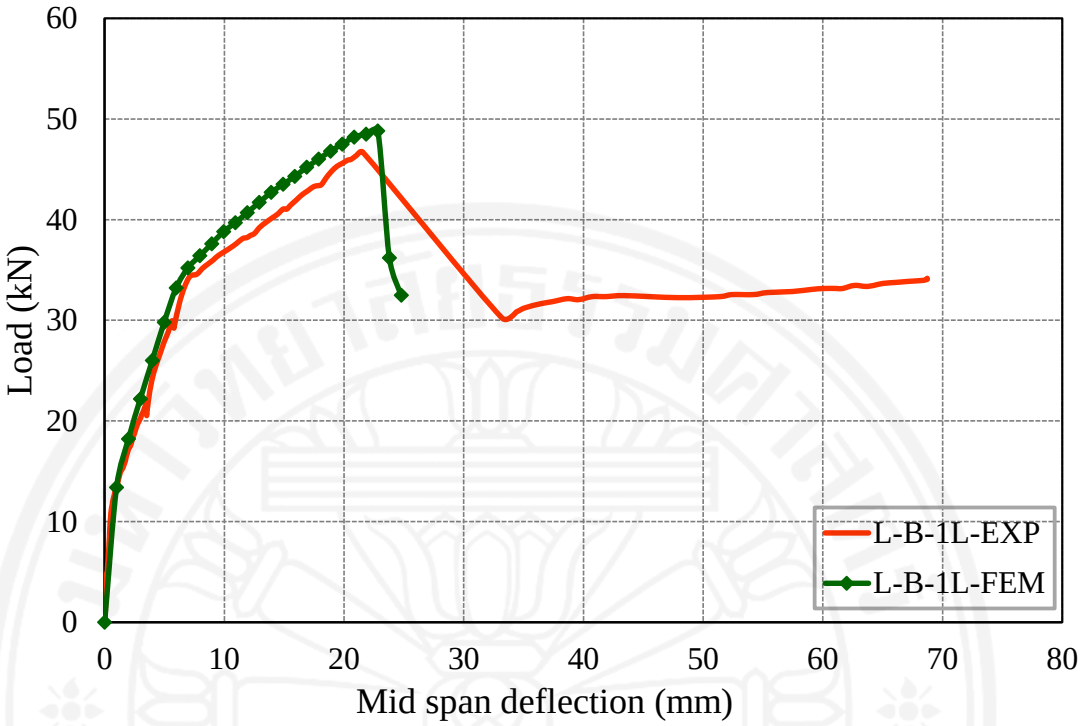
Load (kN)
Mid span deflection (mm)
L-B-1L-EXP
L-B-1L-FEM

(b) L-B-1L

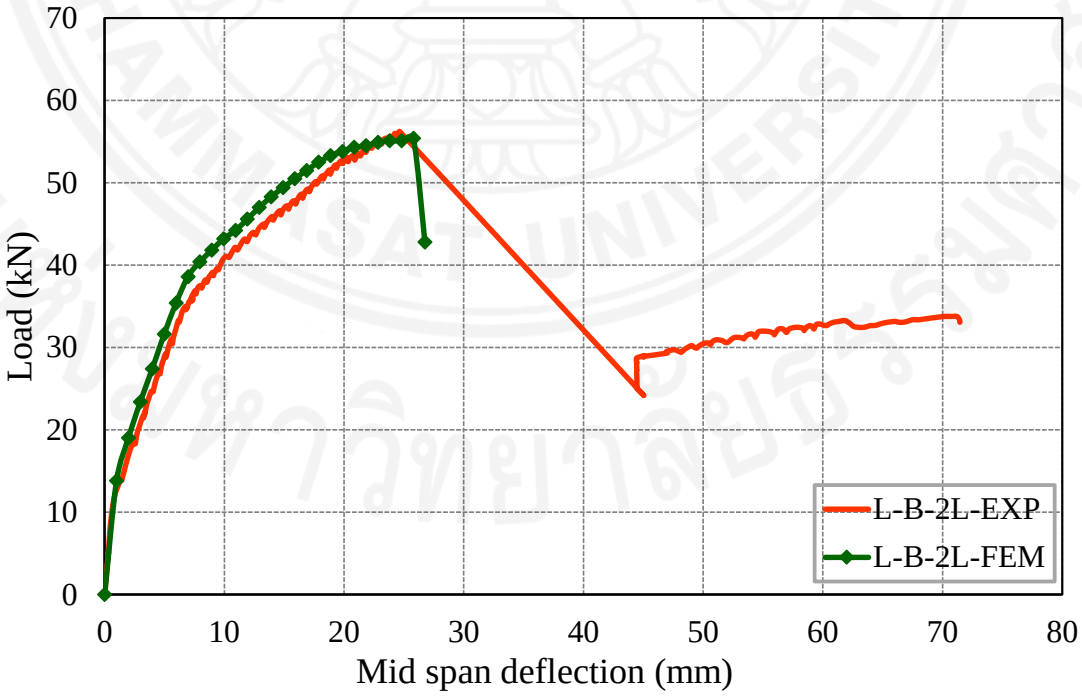
Load (kN)
Mid span deflection (mm)
L-B-2L-EXP
L-B-2L-FEM

(c) L-B-2L

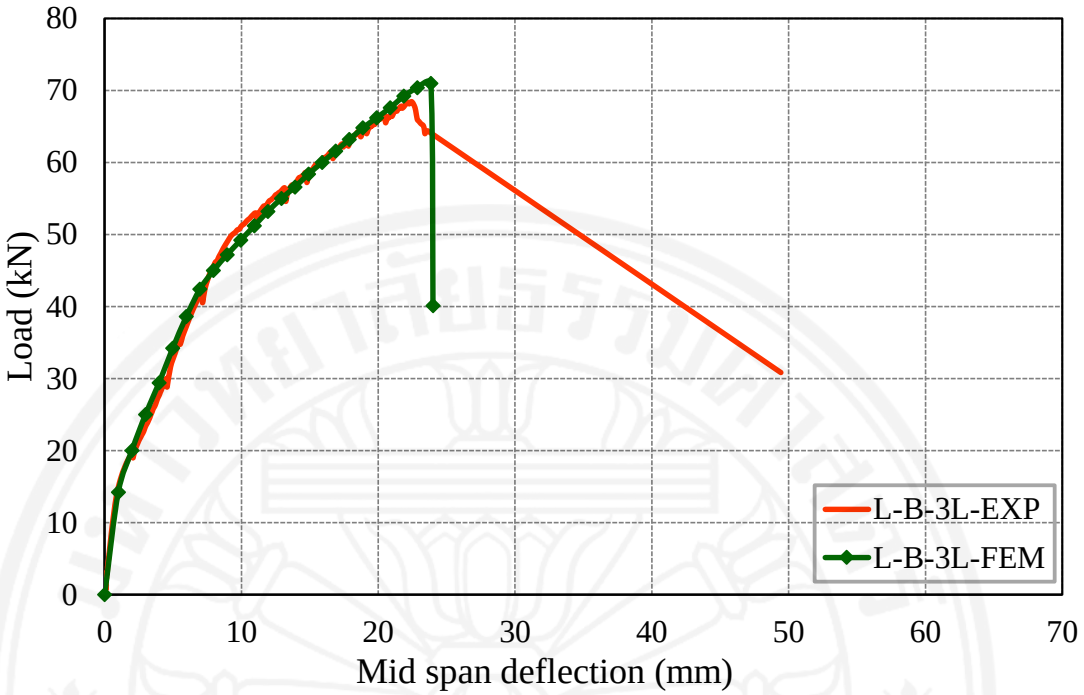
Load (kN)
Mid span deflection (mm)
L-B-3L-EXP
L-B-3L-FEM

(d) L-B-3L

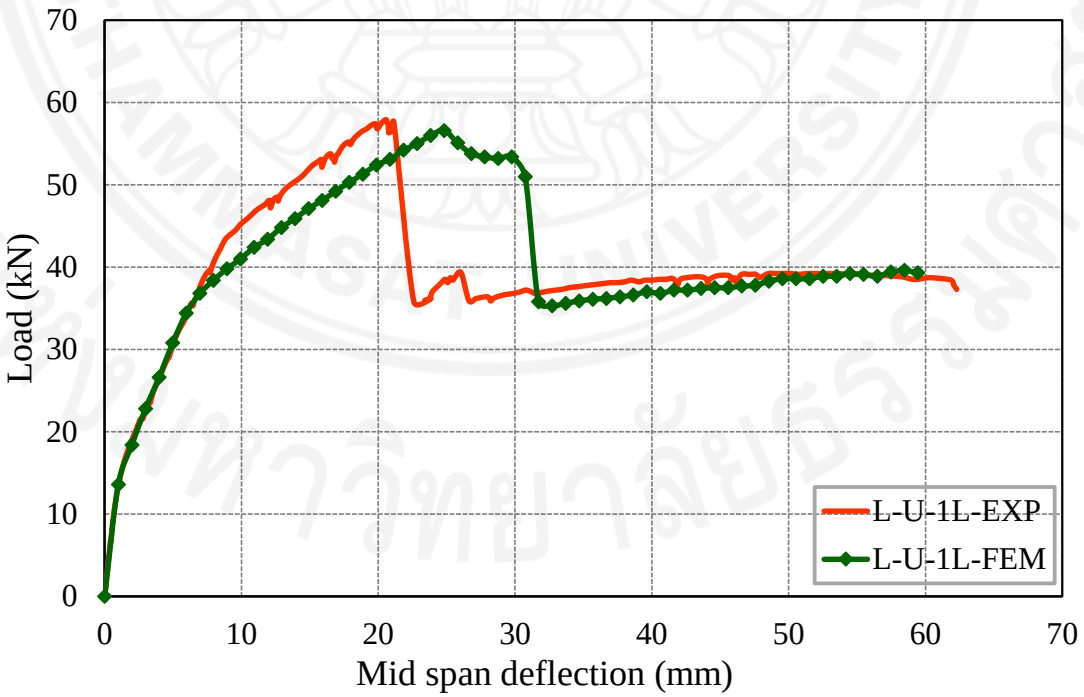
Load (kN)
Mid span deflection (mm)
L-U-1L-EXP
L-U-1L-FEM

(e) L-U-1L

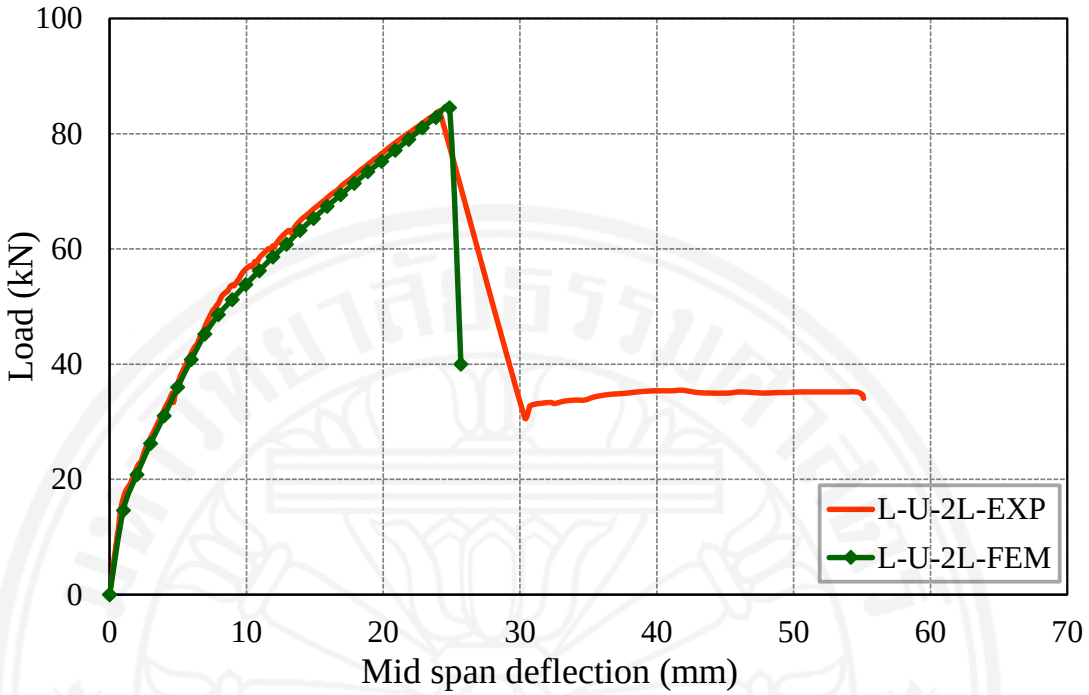

(f) L-U-2L

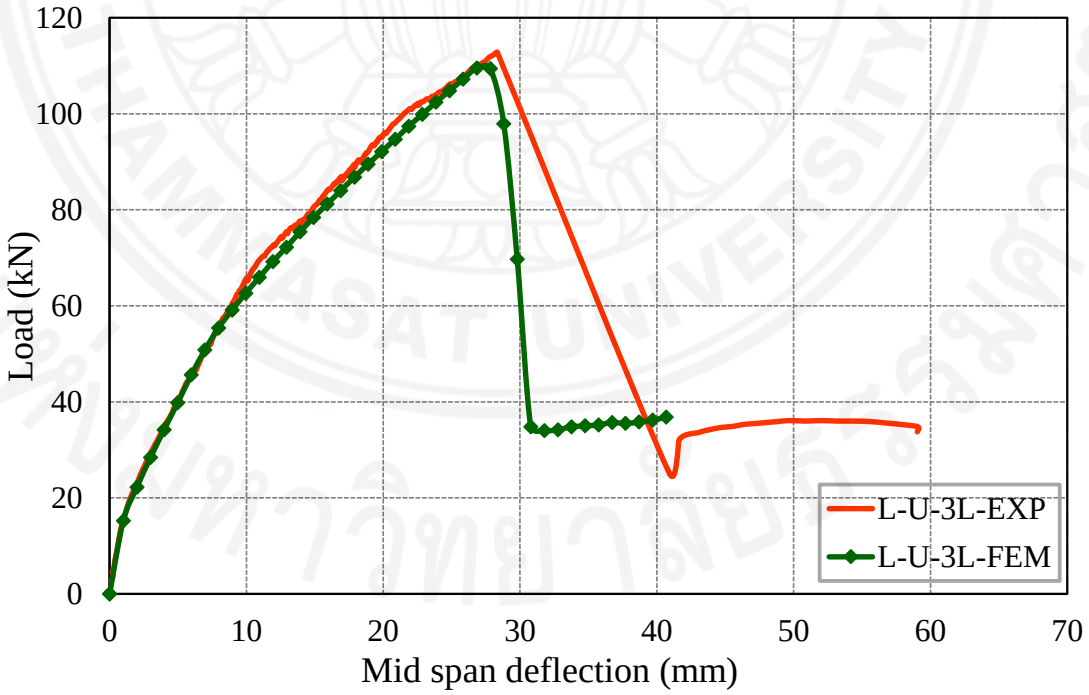

(g) L-U-3L

Figure 8.8 Comparison curves of experimental and analytical results of beam specimens group 1

8.5.2 Specimens group 2

A comparison between experimental and analytical values for selected specimens are summarized and compared in Table 8.5. It can be seen that the results obtained from the VecTor2 were in good accordance with the experimental results. The crack patterns of RC beams observed during testing and the predicted finite lement results are compared as shown in Figure 8.9.

Table 8.5 Summary and comparison of experimental and analytical results of beam specimens group 2

Specimen	Ultimate load (kN)		Analytical/Experimental
	Experimental	Analytical	
H-CON	90.78	89.9	0.99
H-B-2L	95.90	96.5	1.01
H-B-3L	106.3	107.9	1.02
H-U-2L	120.3	126.9	1.05
H-U-3L	131.2	135.2	1.03

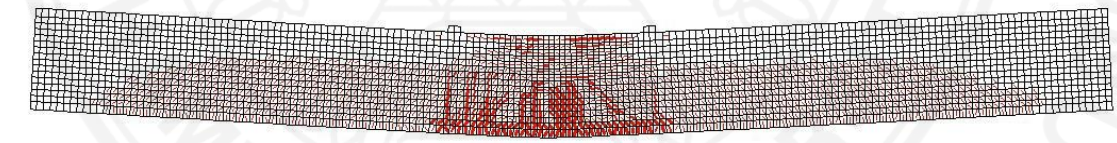

(a) Control beam

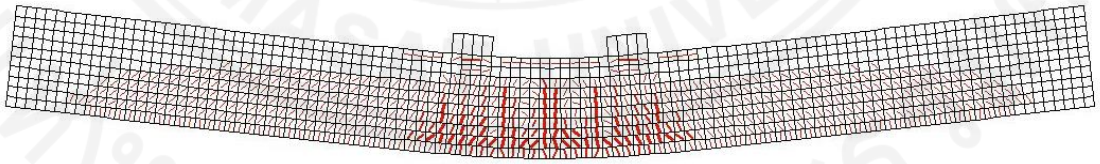

(b) H-B-2L

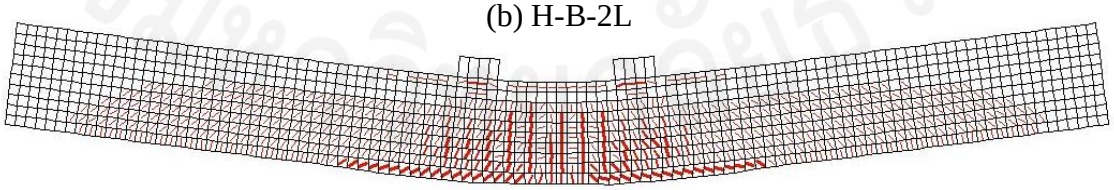

(c) H-U-2L

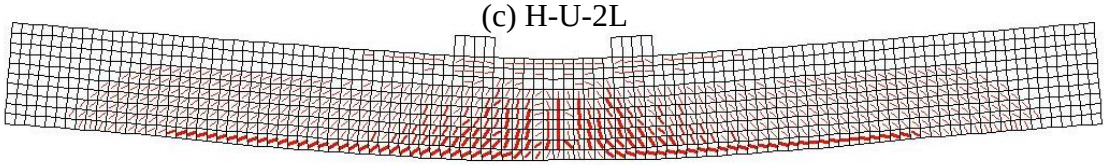

(d) H-U-3L

Figure 8.9 Crack patterns of RC beams group 2

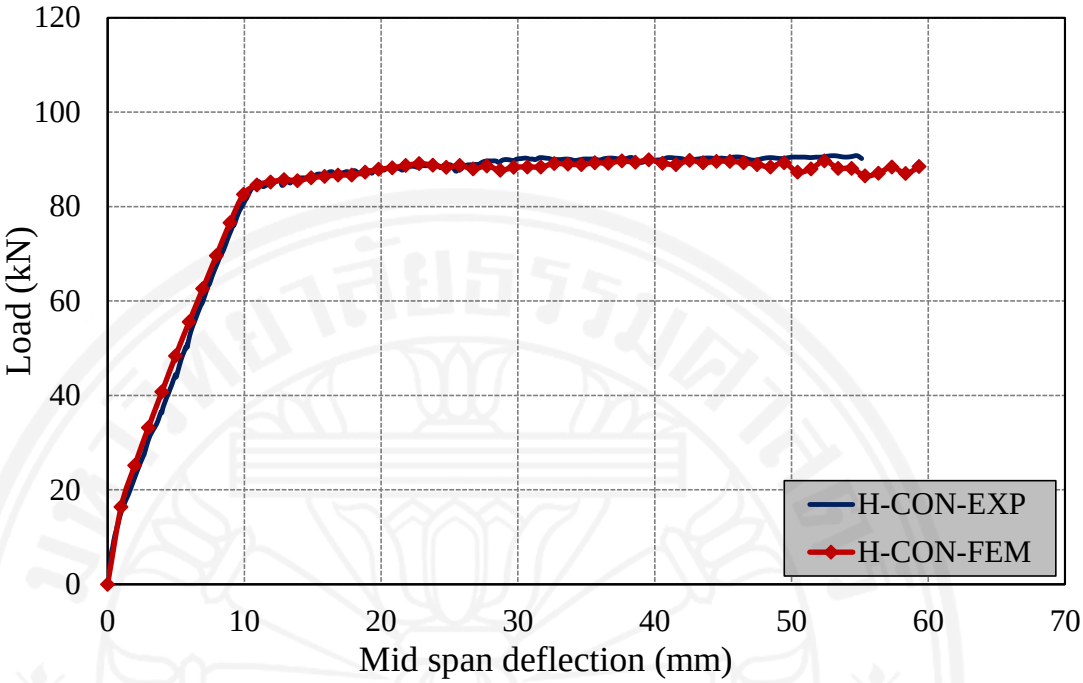

(a) Control beam

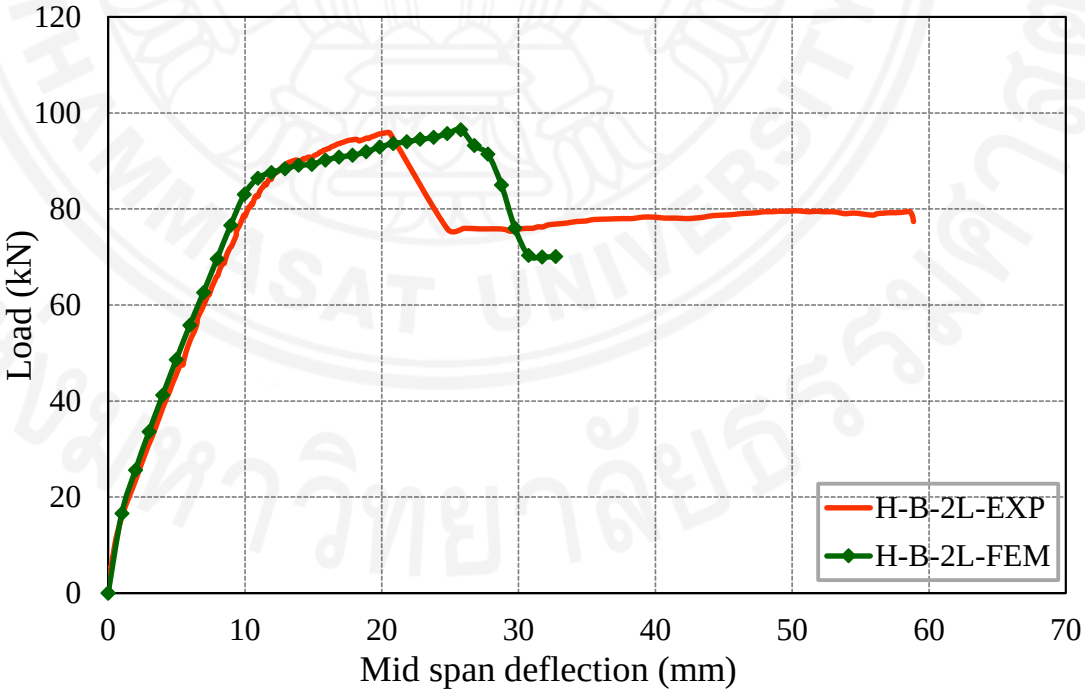

(b) H-B-2L

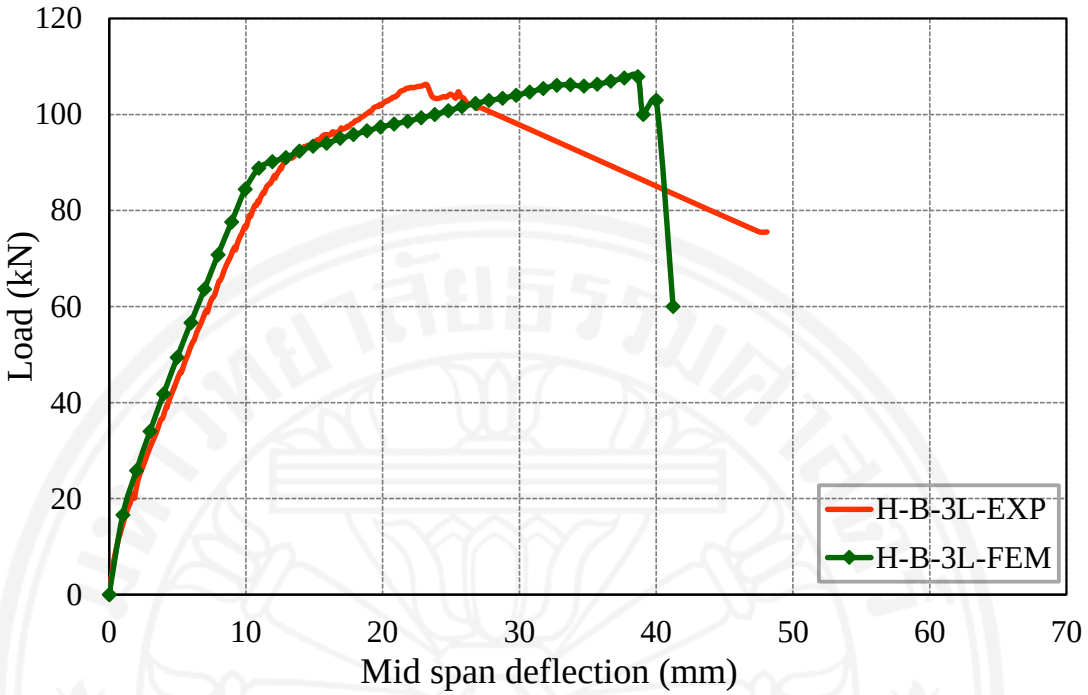
120
100
80
60
40
20
0
Load (kN)
0
10
20
30
40
50
60
70
Mid span deflection (mm)
H-B-3L-EXP
H-B-3L-FEM

(c) H-B-3L

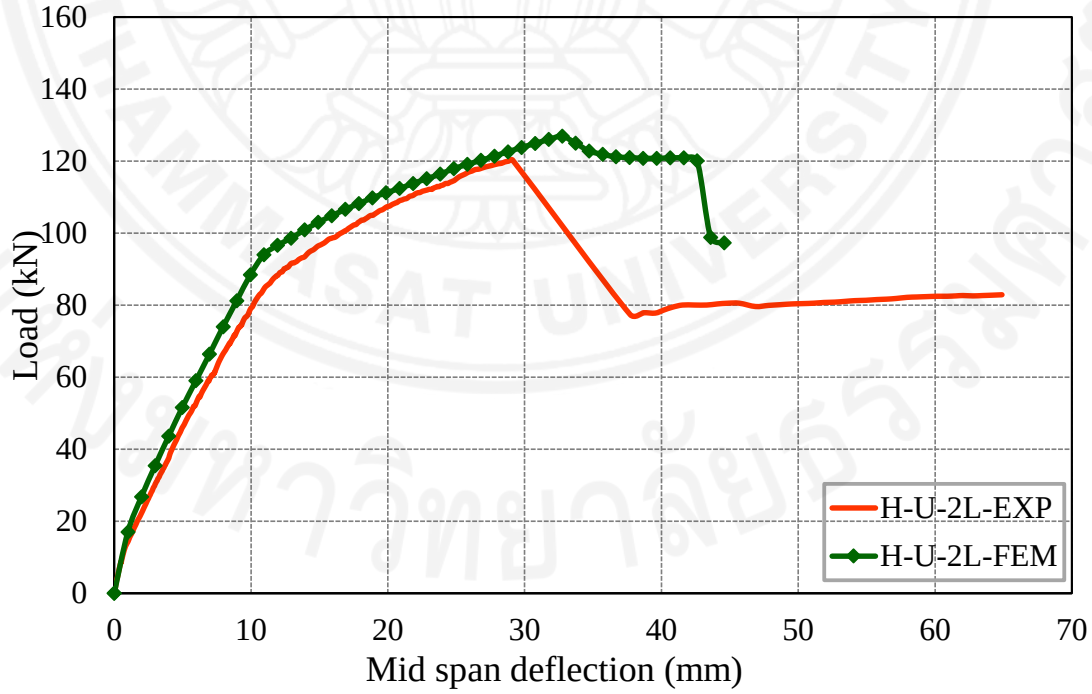
160
140
120
100
80
60
40
20
0
Load (kN)
0
10
20
30
40
50
60
70
Mid span deflection (mm)
H-U-2L-EXP
H-U-2L-FEM

(d) H-U-2L

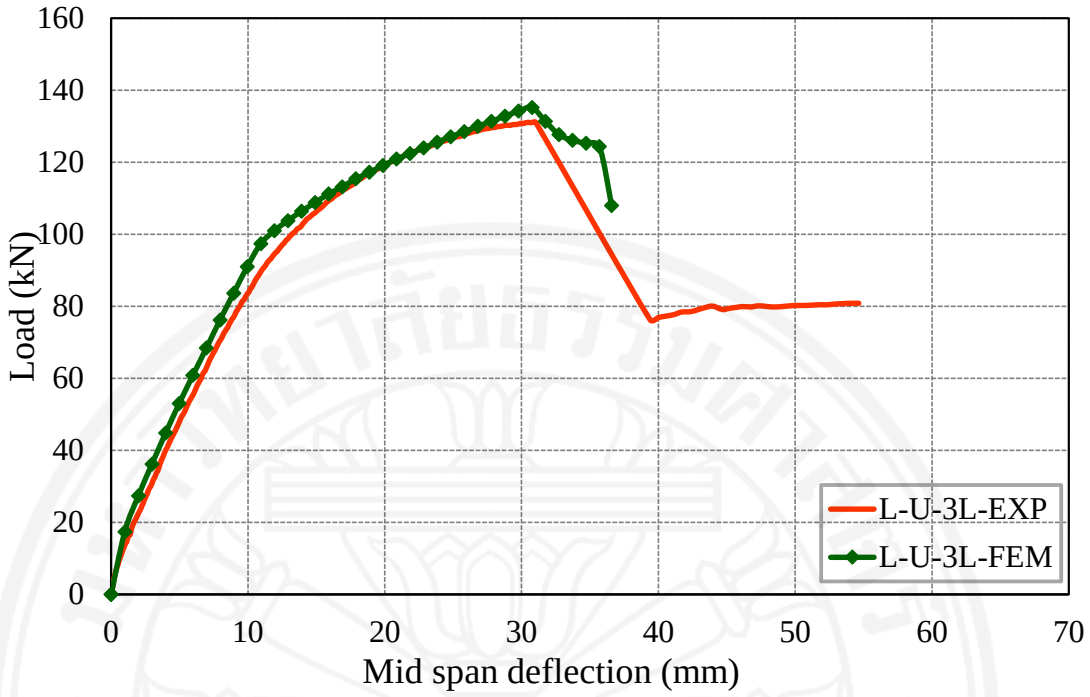

(e) H-U-3L

Figure 8.10 Comparison curves of experimental and analytical results of beam specimens group 2

It can be observed that there is an excellent agreement between the experimental and finite element results until failure. The finite element models can accurately predict the behavior of un-strengthened and hemp FRP strengthened RC beams. The finite element models are also capable of predicting the increase in the ultimate carrying capacity of hemp FRP strengthened RC beams with an increase in fiber thickness and different strengthening configurations. However, it was unable to capture the post-peak behavior of strengthened beams accurately after sudden drop.

Chapter 9
Conclusions and Recommendations

9.1 Conclusions

The experimental results indicated that external bonded strengthening technique using natural fiber composites is an effective method of strengthening existing reinforced concrete (RC) members. This strengthening technique is a feasible method with a suitable low cost, which is an essential goal for the development of reparing and strengthening techniques. Based on the experimental results, the following conclusions can be drawn:

1. Natural fiber reinforced polymer (FRP) composites are found significantly effective to enhance the strength and ductility of confined concrete. The increase in load carrying capacity and ductility is found increasing with natural FRP thickness. The efficiency of natural FRP to provide external confinement and increase in strength is found lower for high strength concrete compared with low strength.
2. Natural FRP bonding to the tension face of both un-reinforced and reinforced concrete beams is found to be effective to increase the flexural strength. The gain in the ultimate flexural strength was more significant in natural FRP strengthened beams using epoxy resin. Natural FRP strengthening reduced the ductility of RC beams due to sudden de-bonding of natural FRP.
3. For strengthening, the epoxy resin is found more effective for natural FRP compared with polyester resin due to better mechanical properties.
4. The proposed end-anchoring system is found to be effective to prevent the delamination of natural FRP from concrete surface to restore the ductility of natural FRP strengthened RC beams.
5. The finite element models can accurately predict the behavior of un-strengthened and hemp FRP strengthened RC beams. The finite element models are also capable to estimate the increase in the ultimate carrying capacity of hemp FRP strengthened RC beams with different strengthening configurations. However, it was unable to capture the post-peak behavior of strengthened beams accurately after sudden drop.

9.2 Recommendations for future research work

For the further studies should be carried out to investigate the behavior of reinforced concrete (RC) beams strengthened using natural FRP in shear. An extensively investigation should be made on RC beams with different shear span-to-depth ratio and the internal stirrup spacing ratio.

References

[1] A. Nanni, "Concrete repair with externally bonded FRP reinforcement," *Concrete International,* vol. 17, 1995.

[2] H. Rahimi and A. Hutchinson, "Concrete beams strengthened with externally bonded FRP plates," *Journal of composites for construction,* vol. 5, pp. 44-56, 2001.

[3] M. Islam, M. Mansur, and M. Maalej, "Shear strengthening of RC deep beams using externally bonded FRP systems," *Cement and Concrete Composites,* vol. 27, pp. 413-420, 2005.

[4] S. V. Joshi, L. Drzal, A. Mohanty, and S. Arora, "Are natural fiber composites environmentally superior to glass fiber reinforced composites?," *Composites Part A: Applied science and manufacturing,* vol. 35, pp. 371-376, 2004.

[5] R. Karnani, M. Krishnan, and R. Narayan, "Biofiber-reinforced polypropylene composites," *Polymer Engineering & Science,* vol. 37, pp. 476-483, 1997.

[6] A. Bledzki and J. Gassan, "Composites reinforced with cellulose based fibres," *Progress in polymer science,* vol. 24, pp. 221-274, 1999.

[7] T. Sen and H. J. Reddy, "Strengthening of RC beams in flexure using natural jute fibre textile reinforced composite system and its comparative study with CFRP and GFRP strengthening systems," *International Journal of Sustainable Built Environment,* vol. 2, pp. 41-55, 2013.

[8] Z. Zhang, C.-T. T. Hsu, and J. Moren, "Shear strengthening of reinforced concrete deep beams using carbon fiber reinforced polymer laminates," *Journal of Composites for Construction,* vol. 8, pp. 403-414, 2004.

[9] S. Cao, J. Chen, J. Teng, Z. Hao, and J. Chen, "Debonding in RC beams shear strengthened with complete FRP wraps," *Journal of Composites for Construction,* vol. 9, pp. 417-428, 2005.

[10] T. C. Triantafillou and C. P. Antonopoulos, "Design of concrete flexural members strengthened in shear with FRP," *Journal of Composites for Construction,* vol. 4, pp. 198-205, 2000.

[11] L. C. Bank, *Composites for construction: structural design with FRP materials*: John Wiley & Sons, 2006.

[12] A. Khalifa, W. J. Gold, A. Nanni, and A. A. MI, "Contribution of externally bonded FRP to shear capacity of RC flexural members," *Journal of Composites for Construction,* vol. 2, pp. 195-202, 1998.

[13] J. Chen and J. Teng, "Anchorage strength models for FRP and steel plates bonded to concrete," *Journal of Structural Engineering,* vol. 127, pp. 784-791, 2001.

[14] J. Chen and J. Teng, "Shear capacity of FRP-strengthened RC beams: FRP debonding," *Construction and Building Materials,* vol. 17, pp. 27-41, 2003.

[15] A. Bousselham and O. Chaallal, "Mechanisms of shear resistance of concrete beams strengthened in shear with externally bonded FRP," *Journal of Composites for Construction,* vol. 12, pp. 499-512, 2008.

[16] O. Chaallal, M. Shahawy, and M. Hassan, "Performance of reinforced concrete T-girders strengthened in shear with carbon fiber-reinforced polymer fabric," *ACI Structural Journal,* vol. 99, 2002.

[17] G. Chen, J. Teng, and J. Chen, "Shear strength model for FRP-strengthened RC beams with adverse FRP-steel interaction," *Journal of Composites for Construction,* vol. 17, pp. 50-66, 2012.
[18] A. Nanni and N. M. Bradford, "FRP jacketed concrete under uniaxial compression," *Construction and Building Materials,* vol. 9, pp. 115-124, 1995.
[19] A. I. Karabinis and T. C. Rousakis, "Carbon FRP confined concrete elements under axial load," in *FRP composites in civil engineering conference*, 2001, pp. 12-15.
[20] T. Norris, H. Saadatmanesh, and M. R. Ehsani, "Shear and flexural strengthening of R/C beams with carbon fiber sheets," *Journal of structural engineering,* vol. 123, pp. 903-911, 1997.
[21] H. Tan, L. Yan, L. Huang, Y. Wang, H. Li, and J. y. Chen, "Behavior of sisal fiber concrete cylinders externally wrapped with jute FRP," *Polymer Composites,* 2015.
[22] A. Ashour, S. El-Refaie, and S. Garrity, "Flexural strengthening of RC continuous beams using CFRP laminates," *Cement and concrete composites,* vol. 26, pp. 765-775, 2004.
[23] R. Kotynia, H. Abdel Baky, K. W. Neale, and U. A. Ebead, "Flexural strengthening of RC beams with externally bonded CFRP systems: Test results and 3D nonlinear FE analysis," *Journal of Composites for Construction,* vol. 12, pp. 190-201, 2008.
[24] D. H. N. J. R. Sandeep kumar L.S, Rumina Nizar "RETROFITTING OF RC BEAMS USING NATURAL FRP WRAPPING (NSFRP) " *International Journal of Emerging trends in Engineering and Development,* vol. 5, pp. 168-178, September 2013.
[25] M. A. R. Bhutta, "Strengthening Reinforced Concrete Beams using Kenaf Fiber Reinforced Polymer Composite Laminates," *Third International Conference on Sustainable Construction Materials and Technologies,* 2013.
[26] M. A. Alam, "Flexural Strengthening of Reinforced Concrete Beam using Jute Rope Composite Plate," *The 3rd National Graduate Conference* pp. 210-213, 2015.
[27] A. D792-00, "Standard Test Methods for Density and Specific Gravity (Relative Density) of Plastics by Displacement," ed. West Conshohocken, PA: ASTM International, 2000.
[28] A. Standard, "D638: Standard Test Method for Tensile Properties of Plastics," *ASTM International, West Conchohocken,* 2008.
[29] A. D2584-11, "Standard Test Method for Ignition Loss of Cured Reinforced Resins," ed. West Conshohocken, PA: ASTM International, 2011.
[30] F. Vecchio, "Disturbed stress field model for reinforced concrete: formulation," *Journal of Structural Engineering,* vol. 126, pp. 1070-1077, 2000.
[31] F. J. Vecchio and M. P. Collins, "The modified compression-field theory for reinforced concrete elements subjected to shear," in *ACI Journal Proceedings*, 1986.
[32] H. Mostafaei, F. Vecchio, and T. Kabeyasawa, "Nonlinear displacement-based response prediction of reinforced concrete columns," *Engineering Structures,* vol. 30, pp. 2436-2447, 2008.

[33] P. Wong and F. Vecchio, "VecTor2 and FormWorks user's manual," *Civil Engineering, University of Toronto, Toronto, Ont*, 2013.